Ocean Engineering 330 (2025) 121117

Contents lists available at ScienceDirect

Ocean Engineering

journal homepage: www.elsevier.com/locate/oceaneng

Research paper

Optimizing ship traffic scheduling in LNG ports: An enhanced model incorporating navigation characteristics and night sailing risks

Shengping Dong [a,b], Guangyao Yang [a,b], Shiguan Liao [c,d,*], Lu Li [e]

[a] School of Transportation and Logistics Engineering, Wuhan University of Technology, Wuhan, 430063, China
[b] State Key Laboratory of Maritime Technology and Safety, Wuhan University of Technology, SKL MTS (WUT), Wuhan, China
[c] School of Management, Shenzhen Polytechnic University, Shenzhen, 518055, China
[d] Maritime Data and Sustainable Development Center, The Hong Kong Polytechnic University, Hung Hom, Kowloon, Hong Kong, China
[e] Department of Logistics and Maritime Studies, The Hong Kong Polytechnic University, Hung Hom, Kowloon, Hong Kong, China

ARTICLE INFO

Keywords:
Ship traffic scheduling
LNG port optimization
Improved simulated annealing genetic algorithm
LNG carrier operations
Night navigation

ABSTRACT

The rapid growth of global liquefied natural gas (LNG) trade and increasing demand for LNG transportation have heightened the need for efficient ship scheduling in ports with LNG facilities. This study addresses these challenges by proposing a mixed-integer linear programming (MILP) model to minimize ship waiting times, incorporating LNG carriers' unique navigation characteristics such as mobile safety zones, one-way navigation, and night navigation risks. An enhanced simulated annealing genetic algorithm (ISAGA) is developed to optimize modeling efficiency. To validate the proposed method, an empirical study was conducted using ship trajectory data from the Dapeng Bay Port Area of Shenzhen as a case study. Findings indicate that allowing nighttime sailing can facilitate the port to accommodate more LNG ships under current berth constraints. Meanwhile, when the port has at least 50 general ship visits and 3 LNG carrier visits, nighttime sailing significantly reduces the waiting time of the ships, and the proposed ISAGA-based approach improves the scheduling efficiency by 22.24 % as compared to the traditional First-Come-First-Served (FCFS) approach. These findings underscore the potential of the proposed method to enhance LNG port operations efficiency, particularly under growing demand.

1. Introduction

Reducing carbon emissions has become a global imperative, with the International Maritime Organization (IMO) requiring that fuel oil used by ships should contain no more than 0.5 % sulphur from 2020 (Yang et al., 2023; Peng et al., 2021). This encourages the transition of the global energy system to cleaner and lower-carbon alternatives. The global demand for liquefied natural gas (LNG), a relatively cleaner fossil fuel that emits fewer pollutants and less carbon dioxide when burned, has grown significantly, further fueling the demand for LNG transportation. International shipping remains the primary mode of transporting LNG, and the demand for LNG ships has continued to rise (Wang et al., 2022; González Gutiérrez et al., 2023). Fig. 1 shows that increasing global LNG trade volumes have driven a corresponding rise in LNG ship traffic and port berthing demands over the past decade.

However, growing LNG ship traffic might exacerbate the congestion and collision risks in ports. LNG ships, as they transport highly flammable and explosive products, have very strict requirements for waterway and port environments, including channel width, water depth, mobile safety zones, and temporary traffic controls (China National Standards, 2021). These safety measures (e.g., channel control, escort operations, safe distance, etc.) can occupy additional waterway resources and restrict the activities of other vessels. The combination of these factors may reduce the overall efficiency of the waterway, especially in port areas where LNG ships frequently enter and exit. In response, some large LNG terminals in China, such as the Shenzhen LNG Terminal, have adopted policies permitting night navigation of LNG carriers to enhance scheduling efficiency. Traditionally, LNG carriers are limited to specific daytime navigation slots, leading to underutilization of port resources and increased waiting times for other ships. By extending navigation to nighttime, LNG carriers can avoid the peak hours during the day and reduce conflicts with other vessels, thus enhancing the overall efficiency of the waterway. On the other hand, lower visibility at night increases navigational risks, especially in complex channels or poor weather conditions, making access to ports and berthing operations more difficult. Therefore, there is a need to

* Corresponding author. School of Management, Shenzhen Polytechnic University, Shenzhen, 518055, China.
E-mail address: sgliao0113@szpu.edu.cn (S. Liao).

https://doi.org/10.1016/j.oceaneng.2025.121117
Received 29 November 2024; Received in revised form 24 March 2025; Accepted 30 March 2025
Available online 16 April 2025
0029-8018/

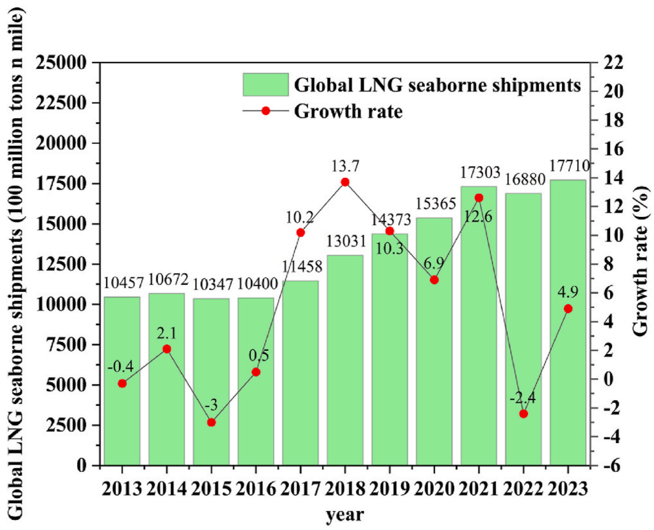

Fig. 1. Global LNG seaborne trade volume trend 2013–2023.

comprehensively assess the impact of allowing LNG vessels to navigate at night on the efficiency of the waterway. Addressing these challenges necessitates integrating LNG carrier navigation characteristics into ship traffic scheduling to improve both safety and efficiency.

This study proposes an optimized ship traffic scheduling method that accounts for night navigation characteristics and sailing risks to facilitate LNG port operations. The method aims to balance navigation safety and scheduling efficiency while addressing the complexities of shared waterways. In most ports and their approach channels, such as Yangshan Port and Putian Port in China, LNG carriers are required to share waterways with other types of vessels. Only a few ports have constructed dedicated LNG channels, such as Dalian port and Caofeidian port in China. Due to the high construction costs and implementation challenges, dedicated LNG channels are rarely adopted (Liu et al., 2019). Therefore, this study focuses on optimizing the efficiency of shared waterways.

Existing research primarily focuses on navigation safety assessments and efficiency analyses for LNG carriers using simulation (Liu et al., 2021a; Zhu et al., 2022) or modeling approaches (Engelen and Dullaert, 2010; Zhou et al., 2017). However, these studies rarely consider LNG carriers' specific navigation characteristics or the practical application of night navigation, limiting their applicability in real-world port operations. Compared to other ships, LNG carriers require a larger mobile safety zone during navigation, which is prohibited to any other ships. All vessels in the fairway opposite to the LNG carrier should anchor or moor before the passage of the LNG carrier to ensure the navigation safety. At night, LNG carriers face additional operational constraints and require wider moving safety zones, lower speeds and longer passage times to safeguard the need for escorts, emergency lighting and other precautions. Although allowing LNG carriers to navigate at night avoids occupying daytime channel resources, a single vessel ties up more channel resources at night than during the day.

To address this gap, this paper innovatively integrates the unique operational constraints of liquefied natural gas (LNG) carriers—such as mobile safety zones, restricted time windows, and port resource limitations—into a comprehensive port ship traffic scheduling framework. We construct a Mixed-Integer Linear Programming (MILP) model that simultaneously considers the safety of LNG carrier navigation and the efficiency of ship traffic scheduling while minimizing total ship waiting times. This dual focus distinguishes our work from previous studies that primarily address either risk assessment or scheduling efficiency in isolation. Furthermore, we develop an improved simulated annealing genetic algorithm (ISAGA) to calculate solutions efficiently, and its effectiveness is validated through comparisons with both the standard genetic algorithm and the CPLEX solver. Empirical analysis based on ship trajectory data from Shenzhen Dapeng Bay Port confirms the superior performance of our method, achieving a 22.24 % improvement in scheduling efficiency over the traditional first-come-first-served (FCFS) approach. The proposed method provides robust decision-making support for port management, particularly under conditions of increasing ship traffic and limited port resources, offering a solid theoretical foundation for optimizing LNG port operations and improving both navigation safety and scheduling efficiency. The proposed method can be adapted and applied to ship traffic scheduling operations in other LNG ports.

The remainder of this paper is organized as follows. Section 2 presents the related research on ship traffic scheduling. Section 3 formulates a mixed-integer linear programming model. Section 4 describes the algorithm. Section 5 exhibits the numerical experiments. Section 6 analyzes the results. Section 7 summarizes the conclusions drawn from this study.

2. Literature review

In this section, we address the central problem of ship traffic scheduling under port resource constraints, specifically focusing on the LNG carrier navigation conditions. To provide a comprehensive overview of the studies related to this issue, we review and analyze three key areas of navigational risks of LNG carriers, ship traffic scheduling with resource constraints, and optimization algorithms for ship traffic scheduling.

2.1. *Navigation risks of LNG carriers*

The navigation risks associated with LNG carriers have been extensively studied. Zhou et al. (2017) developed a modified fault tree model to assess LNG leakage risks during loading and unloading operations, combining fault tree analysis, human reliability analysis, and the Monte Carlo method. Vanem et al. (2008) designed a modular risk assessment model using event tree analysis to identify high-risk areas in LNG maritime operations. Marroni et al. (2023) evaluated LNG carrier navigation risks in vulnerable port areas, emphasizing their proximity to commercial and civilian zones. Similarly, Nwaoha et al. (2013) combined risk matrix and fuzzy evidential reasoning methods to analyze operational risks and their underlying causes. Li and Tang (2019) applied Bayesian belief networks and nonlinear finite element analysis to assess hull damage and LNG leakage risks from grounding incidents. Abdussamie et al. (2018) used a fuzzy set approach to evaluate hazardous scenarios during LNG carrier maneuvers in open seas.

While these studies provide valuable insights into LNG carrier navigation and operational risks, they primarily focus on risk assessment rather than the broader impacts on port resources and other ships. When LNG carriers share port resources (e.g., waterways) with other ships, specific operational requirements such as mobile safety zones and traffic control can delay operations and even cause port congestion. This presents significant challenges for both port security and scheduling efficiency. Furthermore, LNG carriers, due to the hazardous nature of their cargo, often receive higher priority when entering or leaving ports, complicating traffic scheduling decisions. Additionally, night-time operations of LNG carriers, requiring enhanced escort and emergency lighting, increase the complexity of port scheduling—an aspect that has been underexplored in previous research. This highlights the need to integrate LNG carriers' unique navigation characteristics into port traffic scheduling.

2.2. Ship traffic scheduling with resource constraints

Ship traffic scheduling requires consideration of limited port resources, including channels, berths, and anchorages. Liu et al. (2021b) constructed a mixed-integer linear programming model incorporating channel limitations, tidal factors, and berth alignment. Wang et al. (2020) and Zhang et al. (2017) proposed methods addressing restricted two-way channels, while Li et al. (2021a) developed a multi-objective optimization model considering tidal constraints and navigation rules in multi-port basins. Zhang et al. (2024a) examined anchorage-to-terminal channels under drainage restrictions, and Gan et al. (2021) introduced an online scheduling method for restricted channels using a sliding window approach. Jiang et al. (2024) constructed a multi-objective optimization model considering the overall scheduling of constrained channels, berths, and yards in bulk ports. Xia et al. (2023) proposed an integrated ship scheduling method to solve the problem of ship scheduling for unidirectional multi-hub channels in port waters. Zheng et al. (2025) proposed an integrated optimization method considering port ship sequencing and bulk carrier shifting berth configuration.

These studies demonstrate that effective ship traffic scheduling must account for port resource constraints and special conditions such as restricted basins and channel limitations. However, the existing research mainly focuses on general ship traffic scheduling problems and does not fully consider the special navigational requirements of LNG carriers, and more research is needed to address the unique challenges posed by LNG carriers.

2.3. Optimization algorithms for ship traffic scheduling

To effectively solve the ship traffic scheduling problem, researchers have proposed various mathematical optimization models, including mixed integer linear programming (Wu et al., 2022), nonlinear programming (Zhang and Ke, 2024), and multi-objective programming (Dulebenets, 2018). Hill et al. (2019) constructed a mixed integer linear programming model with the objective of minimizing the total waiting time of ships. Meng et al. (2023) constructed a mixed-integer nonlinear planning model considering fuel cost, recycling cost, and carbon emission. Liu et al. (2024a) developed a mixed-integer planning model with the objective of minimizing the total waiting time of a ship at the anchorage for the ship scheduling problem based on channel-lock coordination. In order to obtain the globally optimal solution of the ship traffic scheduling problem, some scholars proposed exact algorithms to solve the ship traffic scheduling model, such as the column generation method (Li et al., 2022) and the branch-and-bound method (Abou Kasm et al., 2021). Li and Jia. (2019) constructed a mixed-integer linear programming model by combining ship traffic scheduling and berth planning, and proposed a column generation algorithm to solve the model. The exact algorithm is effective for large-scale problems, but is computationally intensive and time-consuming.

As a result, heuristic algorithms such as simulated annealing (Jia et al., 2023), particle swarm optimization (Karbassi Yazdi et al., 2020), and variable neighborhood search (Zhang et al., 2024b), offer practical alternatives but face challenges like slow convergence and susceptibility to local optima. To address these limitations, improved heuristic algorithms have been proposed. Examples include the improved grey wolf optimization algorithm (Yao et al., 2024), adaptive genetic simulated annealing (Li et al., 2022), and adaptive multi-objective genetic algorithms (Jiang et al., 2022). These approaches combine optimization mechanisms to enhance solution quality for complex scheduling problems.

2.4. Research gaps and contributions

Despite extensive research on LNG carrier risks, resource-constrained scheduling, and optimization algorithms, current studies often overlook the integration of LNG carriers' navigational characteristics into port scheduling, especially under night-time conditions. LNG carriers are inherently more hazardous due to the nature of their cargo, necessitating the establishment of a strict mobile safety zone around them during their voyage. Additionally, LNG carriers must implement traffic control measures, preventing ships traveling in the opposite direction from navigating during the LNG carrier's passage. Furthermore, LNG carriers require escort ships and emergency lighting. These factors substantially impact the overall efficiency of ship traffic scheduling in LNG ports.

To address these challenges, we build upon existing research and propose a resource-constrained port ship traffic scheduling optimization model that explicitly considers the distinct navigational characteristics of LNG carriers, especially during night-time operations. Unlike previous studies, which typically do not integrate the specific needs of LNG carriers, this study develops a mixed-integer linear programming (MILP) model designed to minimize total ship waiting time while accounting for the unique navigational constraints of LNG carriers and the limitations of port resources. This model provides a comprehensive solution to the practical challenges faced by LNG ports, significantly improving scheduling efficiency and safety. An improved simulated annealing genetic algorithm (ISAGA) is proposed to solve the model efficiently. Case studies using data from Shenzhen Dapeng Bay Port demonstrate the method's superiority over traditional first-come-first-served (FCFS) scheduling, offering practical and theoretical support for improving port scheduling efficiency and safety.

3. Problem description and formulation

3.1. Problem description

Ship traffic scheduling is designed to rationally arrange the sequence and time of ships' entry and exit from the waterway, achieve efficient utilization of resources such as waterways and berths, and enhance port operation efficiency (Gan et al., 2021). Unlike other types of ships, LNG carriers typically require significant resources during their navigation, which includes the establishment of mobile safety zones. While other ships only need to maintain a safe distance, LNG carriers have strict no-entry mobile safety zones around them. Furthermore, LNG carriers enforce traffic control measures such as one-way navigation, where the opposite channel must be cleared of all traffic during the LNG carrier's

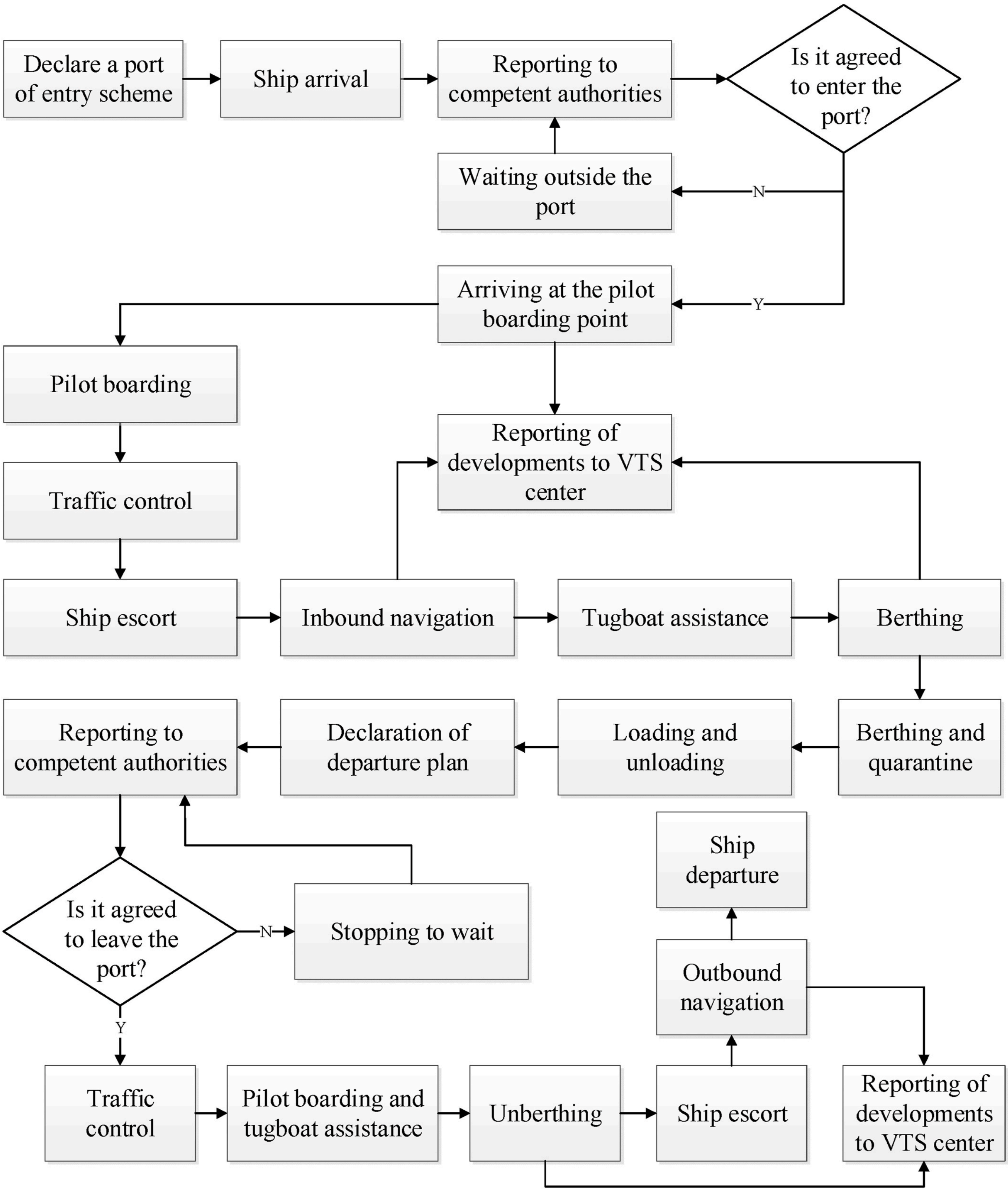

Fig. 2. Flowchart of traffic organization for LNG carriers entering and leaving the port.

passage. These operational requirements create unique challenges that impact traditional ship traffic scheduling strategies. It is worth noting that LNG carriers are also different from other types of ships when navigating at night, with the additional requirements for escort and emergency lighting requiring extended mobile safety zones and reduced speeds. This further prolongs their time in-port and adversely affects the overall efficiency of ship traffic scheduling. Therefore, devising an effective port ship traffic scheduling solution that accounts for the unique navigational characteristics of LNG carriers is a complex and pressing challenge for port managers.

In the actual operation of the port, the navigation and operation process of LNG carriers in and out of the port mainly includes: declare a port of entry scheme, ship arrival, traffic control, channel inbound navigation, berthing operation, end of traffic control, loading and unloading operation at the terminal, declaration of outbound plan, traffic control, unberthing operation, channel outbound navigation, end of traffic control, ship departure from the port, as shown in Fig. 2.

The ship traffic scheduling problem in this paper can be described as follows: Given the known moments when ships apply for entry and exit from the port, taking all ships expected to arrive at and depart from the port within a fixed planning period as the research objects, with a particular focus on the special circumstances arising when the port is open to the navigation of LNG carriers. The unique navigational requirements of LNG carriers include: (1) traffic control. In two-way fairways, when traffic control is implemented, ships traveling in the opposite direction must wait at anchorage or berth until the LNG carrier's voyage is completed; (2) Mobile safety zone: During LNG carrier navigation, no other ships are allowed to enter its mobile safety zone; (3) Priority for entry and exit. Due to the hazardous nature of the cargoes transported by LNG carriers, they are granted higher priority when entering or exiting the port; (4) Night navigation: At night, LNG carriers require special escort services, emergency lighting, and other operational measures. Furthermore, compared to daytime navigation, the mobile safety zone of LNG carriers is larger, and their navigational speed is lower. Based on these unique characteristics, a mixed-integer linear programming model is developed with the objective of minimizing the total waiting time for all ships entering and exiting the port. Notably, the ship traffic scheduling model constructed in this paper is based on the truly statistically collected ship navigation trajectory data, without considering the impact of possible unknown factors on ship traffic scheduling.

3.2. Assumptions

To facilitate modeling and solution, the following assumptions are made regarding the navigation conditions of LNG carriers:

(1) Except for LNG carriers that are allowed for night navigation, the time window for LNG carriers to enter and exit the port daily is from 8:00 a.m. to 18:00 p.m.
(2) LNG carriers meet the requirements of navigational environment when entering and leaving ports, berthing and navigating at night.
(3) When LNG carriers apply for entry and exit from the port, there are sufficient resources such as pilots and tugboats.
(4) LNG carriers have dedicated berths and meet the requirements for the layout of dangerous goods berths.

3.3. Parameter meaning

Before formulating the model for this problem, the notations related to the ship traffic scheduling problem are defined:

Indices and sets:
E: set of all inbound and outbound ships, we use the index $i \in \mathrm{E}$.
E^{in}: set of all inbound ships other than LNG carriers.
E^{out}: set of all outbound ships other than LNG carriers.
E^{inlng}: set of inbound LNG carriers within the sailing time window.
E^{outlng}: set of outbound LNG carriers within the sailing time window.
E^{tolng}: set of inbound LNG carriers with night sailing capability.
$\mathrm{E}^{leavelng}$: set of outbound LNG carriers with night sailing capability.
H: set of inbound and outbound ship types, ship type $h \in H$.
A: set of anchorages, anchorage $a \in A$.
B: set of berths, berth $b \in B$.
Υ: set of periods for the planning cycle, $t \in \Upsilon$.
Υ_i: total time for ship i to complete inbound or outbound operations.
Υ^{day}: set of time within the sailing time window of LNG carriers.
Υ^{night}: set of time outside the sailing time window of LNG carriers.
Parameters:
w_i^{app}: time of ship i application for entry and leave port (*min*).
$\Phi_a^{entrance}$: distance from anchorage a to channel entrance (*n mile*).
Φ_a^{outlet}: distance from anchorage a to channel exit (*n mile*).
$\Phi_{a,b}^{sail}$: distance from anchorage a to berth b (*n mile*).
Φ^{inout}: distance from channel entrance to channel exit (*n mile*).
Φ_b^{exit}: distance from channel exit to berth b (*n mile*).
$\psi(t)$: ship scheduling time as a function of ship scheduling moment t (*min*).
$v_i^{average}$: average speed of ship i (*knot*).
χ^{safe}: minimum safe time intervals for ships (*min*).
χ^{besafe}: minimum safe time intervals for night-capable LNG carriers (*min*).
δ_h: number of berths for type h ships in the port (*berth*).
δ_h^{begin}: the number of ships of type h docked at the port at the beginning of the planning cycle (*ship*).
$\Gamma_a^{\max}$: Anchorage a maximum number of ships at anchor (*ship*).
$\theta_{i,h}^{priority}$: priority factor of inbound or outbound ship i of type h.
Intermediate variables:
$\beta_{t,a}$: anchorage a number of ships at anchor at time t (*ship*).
η_i^{outer}: time of inbound ship i from the outer anchorage to channel entrance (*min*).
η_i^{inout}: time of inbound ship i from channel entrance to channel exit or time of outbound ship i from channel exit to channel entrance (*min*).
η_i^{berth}: time of inbound ship i from channel exit to the berth or outbound ship i from the berth to channel exit (*min*).
η_i^{inner}: time of inbound ship i from channel exit to the inner anchorage or outbound ship i from the inner anchorage to channel exit (*min*).
$\eta_i^{arrival}$: time of inbound ship i from the inner anchorage to the berth or outbound ship i from the berth to the inner anchorage (*min*).
Decision variables:
$x_{i,h,t} \in \{0,1\}$: 1 if ship i of type h starts inbound or outbound operations at time t; 0 otherwise.
$\varsigma_{i,j} \in \{0,1\}$: 1 if the priority factor of ship i higher than ship j, $i,j \in \mathrm{E}$; 0 otherwise.
$\varepsilon_{i,h,t} \in \{0,1\}$: 1 if the number of free berths for ship i of type h at time t is not 0; 0 otherwise.
Variables:
$Z \geq 0$: total waiting time of ships (*min*).
$w_i^{act} \geq 0$: actual time when ship i enter or leave the port (*min*).

Regarding the abbreviation used in this paper, n mile denotes Nautical Mile. We use this abbreviation consistently throughout the paper.

3.4. Mixed-integer linear programming model

Based on the above description, the specific details of the model established in this paper are as follows:

The general ship scheduling model can be described as follows:

Objective Function:

$$\min Z = \sum_{i \in \mathrm{E}} \left(w_i^{act} - w_i^{app} \right) \tag{1}$$

The objective is subject to the following constraints:

$$w_i^{act} \geq w_j^{act} + \chi^{safe}, \forall i,j \in \mathrm{E}^{in} \cup \mathrm{E}^{inlng}, v_j^{average} \geq v_i^{average}, w_i^{act} \geq w_j^{act}, i \neq j \tag{2}$$

$$w_i^{act} + \eta_i^{outer} + \eta_i^{inout} + x_{i,h,t} \cdot \eta_i^{berth} + (1 - x_{i,h,t})(\eta_i^{inner} + \eta_i^{arrival}) \geq w_j^{act} + \eta_j^{outer} + \eta_j^{inout} + x_{j,h,t} \cdot \eta_j^{berth} + (1 - x_{j,h,t})\left(\eta_j^{inner} + \eta_j^{arrival}\right) + \chi^{safe}, \forall i,j \in \mathrm{E}^{in} \cup \mathrm{E}^{inlng}, v_i^{average} \geq v_j^{average}, w_i^{act} \geq w_j^{act}, i \neq j \tag{3}$$

$$w_i^{act} \geq w_j^{act} + \chi^{safe}, \forall i,j \in \mathrm{E}^{out} \cup \mathrm{E}^{outlng}, v_j^{average} \geq v_i^{average}, w_i^{act} \geq w_j^{act}, i \neq j \tag{4}$$

$$w_i^{act} + \eta_i^{inout} + x_{i,h,t} \cdot \eta_i^{berth} + (1 - x_{i,h,t})(\eta_i^{inner} + \eta_i^{arrival}) \geq w_j^{act} + \eta_j^{inout} + x_{j,h,t} \cdot \eta_j^{berth} + (1 - x_{j,h,t})\left(\eta_j^{inner} + \eta_j^{arrival}\right) + \chi^{safe}, \forall i,j \in \mathrm{E}^{out} \cup \mathrm{E}^{outlng}, v_i^{average} \geq v_j^{average}, w_i^{act} \geq w_j^{act}, i \neq j \tag{5}$$

$$w_i^{act} \geq w_i^{app}, \forall i \in \mathrm{E} \tag{6}$$

$$\beta_{t,a} \leq \Gamma_a^{\max}, \forall t \in \Upsilon, a \in A \tag{7}$$

$$\psi(t) = \max\{\min\{t, |\Upsilon|\}, 0\} \tag{8}$$

$$w_i^{act} \geq w_j^{act} + \chi^{besafe}, \forall i,j \in \mathrm{E}^{in} \cup \mathrm{E}^{inlng} \cup \mathrm{E}^{tolng}, v_j^{average} \geq v_i^{average}, w_i^{act} \geq w_j^{act}, i \neq j \tag{9}$$

$$w_i^{act} + \eta_i^{outer} + \eta_i^{inout} + x_{i,h,t} \cdot \eta_i^{berth} + (1 - x_{i,h,t})(\eta_i^{inner} + \eta_i^{arrival}) \geq w_j^{act} + \eta_j^{outer} + \eta_j^{inout} + x_{j,h,t} \cdot \eta_j^{berth} + (1 - x_{j,h,t})\left(\eta_j^{inner} + \eta_j^{arrival}\right) + \chi^{besafe}, \forall i,j \in \mathrm{E}^{in} \cup \mathrm{E}^{inlng} \cup \mathrm{E}^{tolng}, v_i^{average} \geq v_j^{average}, w_i^{act} \geq w_j^{act}, i \neq j \tag{10}$$

$$w_i^{act} \geq w_j^{act} + \chi^{besafe}, \forall i,j \in \mathrm{E}^{out} \cup \mathrm{E}^{outlng} \cup \mathrm{E}^{leavelng}, v_j^{average} \geq v_i^{average}, w_i^{act} \geq w_j^{act}, i \neq j \tag{11}$$

$$w_i^{act} + \eta_i^{inout} + x_{i,h,t} \cdot \eta_i^{berth} + (1 - x_{i,h,t})(\eta_i^{inner} + \eta_i^{arrival}) \geq w_j^{act} + \eta_j^{inout} + x_{j,h,t} \cdot \eta_j^{berth} + (1 - x_{j,h,t})\left(\eta_j^{inner} + \eta_j^{arrival}\right) + \chi^{besafe}, \forall i,j \in \mathrm{E}^{out} \cup \mathrm{E}^{outlng} \cup \mathrm{E}^{leavelng}, v_i^{average} \geq v_j^{average}, w_i^{act} \geq w_j^{act}, i \neq j \tag{12}$$

$$\eta_i^{outer} = \Phi_a^{entrance} \div v_i^{average}, \forall i \in \mathrm{E}^{in}, a \in A \tag{13}$$

$$\eta_i^{inout} = \Phi^{inout} \div v_i^{average}, \forall i \in \mathrm{E} \tag{14}$$

$$\eta_i^{berth} = \Phi_b^{exit} \div v_i^{average}, \forall i \in \mathrm{E}, b \in B \tag{15}$$

$$\eta_i^{inner} = \Phi_a^{outlet} \div v_i^{average}, \forall i \in \mathrm{E}, a \in A \tag{16}$$

$$\eta_i^{arrival} = \Phi_{a,b}^{sail} \div v_i^{average}, \forall i \in \mathrm{E}, a \in A, b \in B \tag{17}$$

$$\Upsilon_i = \eta_i^{outer} + \eta_i^{inout} + x_{i,h,t}\eta_i^{berth} + (1 - x_{i,h,t})(\eta_i^{inner} + \eta_i^{arrival}), \forall i \in \mathrm{E}^{in} \cup \mathrm{E}^{inlng} \cup \mathrm{E}^{tolng}, t \in \Upsilon, h \in H \tag{18}$$

$$\Upsilon_i = \eta_i^{inout} + x_{i,h,t}\eta_i^{berth} + (1 - x_{i,h,t})(\eta_i^{inner} + \eta_i^{arrival}), \forall i \in \mathrm{E}^{out} \cup \mathrm{E}^{outlng} \cup \mathrm{E}^{leavelng}, t \in \Upsilon, h \in H \tag{19}$$

$$\delta_h \geq \delta_h^{begin} + \sum_{i \in \mathrm{E}^{in} \cup \mathrm{E}^{inlng} \cup \mathrm{E}^{tolng}, i=1}^{\left|\mathrm{E}^{in} + \mathrm{E}^{inlng} + \mathrm{E}^{tolng}\right|} \sum_{t=0}^{\psi(t)} x_{i,h,t} - \sum_{j \in \mathrm{E}^{out} \cup \mathrm{E}^{outlng} \cup \mathrm{E}^{leavelng}, j=1}^{\left|\mathrm{E}^{out} + \mathrm{E}^{outlng} + \mathrm{E}^{leavelng}\right|} \times \sum_{t'=0}^{\psi(t)} x_{j,h,t}, \forall t \in \Upsilon, h \in H \tag{20}$$

$$\begin{cases} x_{i,h,t} = 0, otherwise \\ x_{i,h,t} = 1, \varepsilon_{i,h,t} = 1, w_i^{act} = t \end{cases}, \forall i \in \mathrm{E}^{in} \cup \mathrm{E}^{inlng} \cup \mathrm{E}^{tolng}, t \in \Upsilon, h \in H \tag{21}$$

$$\begin{cases} \varsigma_{i,j} = 0, otherwise \\ \varsigma_{i,j} = 1, \theta_{i,h}^{priority} > \theta_{j,h}^{priority} \end{cases}, \forall i, j \in \mathrm{E}^{in} \cup \mathrm{E}^{inlng} \cup \mathrm{E}^{tolng}, h \in H, i \neq j \tag{22}$$

$$\begin{cases} \varsigma_{i,j} = 0, otherwise \\ \varsigma_{i,j} = 1, \theta_{i,h}^{priority} > \theta_{j,h}^{priority} \end{cases}, \forall i, j \in \mathrm{E}^{out} \cup \mathrm{E}^{outlng} \cup \mathrm{E}^{leavelng}, h \in H, i \neq j \tag{23}$$

$$\begin{cases} \varepsilon_{i,h,t} = 0, otherwise \\ \varepsilon_{i,h,t} = 1, \delta_h - \delta_h^{begin} - \sum_{i \in \mathrm{E}^{in} \cup \mathrm{E}^{inlng} \cup \mathrm{E}^{tolng}, i=1}^{\left|\mathrm{E}^{in} + \mathrm{E}^{inlng} + \mathrm{E}^{tolng}\right|} \sum_{t=0}^{\psi(t)} x_{i,h,t} + \sum_{j \in \mathrm{E}^{out} \cup \mathrm{E}^{outlng} \cup \mathrm{E}^{leavelng}, j=1}^{\left|\mathrm{E}^{out} + \mathrm{E}^{outlng} + \mathrm{E}^{leavelng}\right|} \sum_{t'=0}^{\psi(t)} x_{j,h,t} > 0 \end{cases}, \forall t \in \Upsilon, h \in H \tag{24}$$

$$x_{i,h,t}, \varsigma_{i,j}, \varepsilon_{i,h,t} = 0, 1, \forall i, j \in \mathrm{E}, t \in \Upsilon, h \in H \tag{25}$$

Eq. (1) represents the objective function, which is to minimize the total waiting time of ships. Constraints (2)–(5) ensure that two ships sailing in the same direction maintain a safe time interval during the entry and exit operations and no overtaking occurs. Constraint (6) guarantees that the actual start time of a ship's entry and exit operation is not less than the start time of the application for entry and exit operation. Constraint (7) indicates that the number of ships waiting at the anchorage within the planning period shall not exceed the upper limit of the number of ships that can wait at the anchorage. Constraint (8) ensures that the completion time of a ship's entry and exit operation does not exceed the total planned time. Constraints (9)–(12) ensure that night-capable LNG carriers always maintain a safe time interval and no overtaking occurs during the navigation with ships in the same direction. Eq. (13)–(19) ensure the time continuity of ships' entry and exit navigation. Constraint (20) guarantees that the number of used berths of each type does not exceed the total number of berths of each type. Constraint (21) ensures that a ship of a certain type can start the entry operation only when the berth is available. Constraints (22)–(23) determine the priority of ships i and j for entry or exit. Constraint (24) determines whether there is a free berth for ship i of type h to berth at time t. Constraint (25) specifies the binary variable.

The ship scheduling model with further consideration of the navigation characteristics of LNG carriers is depicted as follows:

$$\begin{cases} 1080 + 1440n \geq w_i^{act} \geq 480 + 1440n \\ 1080 + 1440n \geq w_i^{act} + \eta_i^{inout} + \eta_i^{berth} \geq 480 + 1440n \end{cases}, \forall i \in \mathrm{E}^{inlng} \cup \mathrm{E}^{outlng}, n = 0, 1, \ldots, n-1 \tag{26}$$

$$\sum_{t=\psi\left(w_i^{act}\right)}^{\psi\left(w_i^{act}+\eta_i^{inout}+\eta_i^{berth}\right)} \left(x_{i,h,t} + x_{j,h,t}\right) \leq 1, i \in \mathrm{E}^{inlng} \cup \mathrm{E}^{tolng}, j \in \mathrm{E}^{out} \cup \mathrm{E}^{outlng} \cup \mathrm{E}^{leavelng}, h \in H \tag{27}$$

$$\sum_{t=\psi\left(w_i^{act}\right)}^{\psi\left(w_i^{act}+\eta_i^{inout}+\eta_i^{berth}\right)} \left(x_{i,h,t} + x_{j,h,t}\right) \leq 1, i \in \mathrm{E}^{outlng} \cup \mathrm{E}^{leavelng}, j \in \mathrm{E}^{in} \cup \mathrm{E}^{inlng} \cup \mathrm{E}^{tolng}, h \in H \tag{28}$$

$$\begin{cases} x_{i,h,t} = 0, otherwise \\ x_{i,h,t} = 1, \varsigma_{i,j} = 1, w_i^{act} = w_j^{act} = t \end{cases}, \forall i, j \in \mathrm{E}^{in} \cup \mathrm{E}^{inlng} \cup \mathrm{E}^{tolng}, t \in \Upsilon^{day}, h \in H, i \neq j \tag{29}$$

$$\begin{cases} x_{i,h,t} = 0, otherwise \\ x_{i,h,t} = 1, \varsigma_{i,j} = 1, w_i^{act} = w_j^{act} = t \end{cases}, \forall i, j \in \mathrm{E}^{out} \cup \mathrm{E}^{outlng} \cup \mathrm{E}^{leavelng}, t \in \Upsilon^{day}, h \in H, i \neq j \tag{30}$$

$$\begin{cases} x_{i,h,t} = 0, otherwise \\ x_{i,h,t} = 1, \varsigma_{i,j} = 1, w_i^{act} = w_j^{act} = t \end{cases}, \forall i, j \in \mathrm{E}^{in} \cup \mathrm{E}^{tolng}, t \in \Upsilon^{night}, h \in H, i \neq j \tag{31}$$

$$\begin{cases} x_{i,h,t} = 0, otherwise \\ x_{i,h,t} = 1, \varsigma_{i,j} = 1, w_i^{act} = w_j^{act} = t \end{cases}, \forall i, j \in \mathrm{E}^{out} \cup \mathrm{E}^{leavelng}, t \in \Upsilon^{night}, h \in H, i \neq j \tag{32}$$

To account for the specific sailing time window required for LNG carriers, construct the Constraint (26) ensures that the actual start and end times of LNG carriers' operations are within the daytime range. Here, n represents the number of planned days; for example, when the planned days are 3, $n = 0,1,2$. Furthermore, the traffic control measures associated with LNG carrier navigation are crucial. During LNG carrier operations, no ships are allowed to sail in the opposite direction within the designated fairway. To enforce this, Constraints (27)–(28) ensure that there is no opposite-direction ship sailing when LNG carriers enter or exit the port. Based on the high priority of LNG carriers when entering and leaving ports, Constraints (29)–(30) indicate that during the daytime, when the actual entry and exit times of LNG carriers are the same as those of other ships, the entry and exit operations of LNG carriers are given priority; Constraints (31)–(32) state that outside the daytime, when the actual entry and exit times of LNG carriers are the same as those of other ships, the entry and exit operations of LNG carriers are also given priority. Moreover, the special requirements of LNG carriers regarding their mobile safety zones during navigation are reflected in Constraints (2)–(5) and (9)–(12), LNG carriers always maintain the

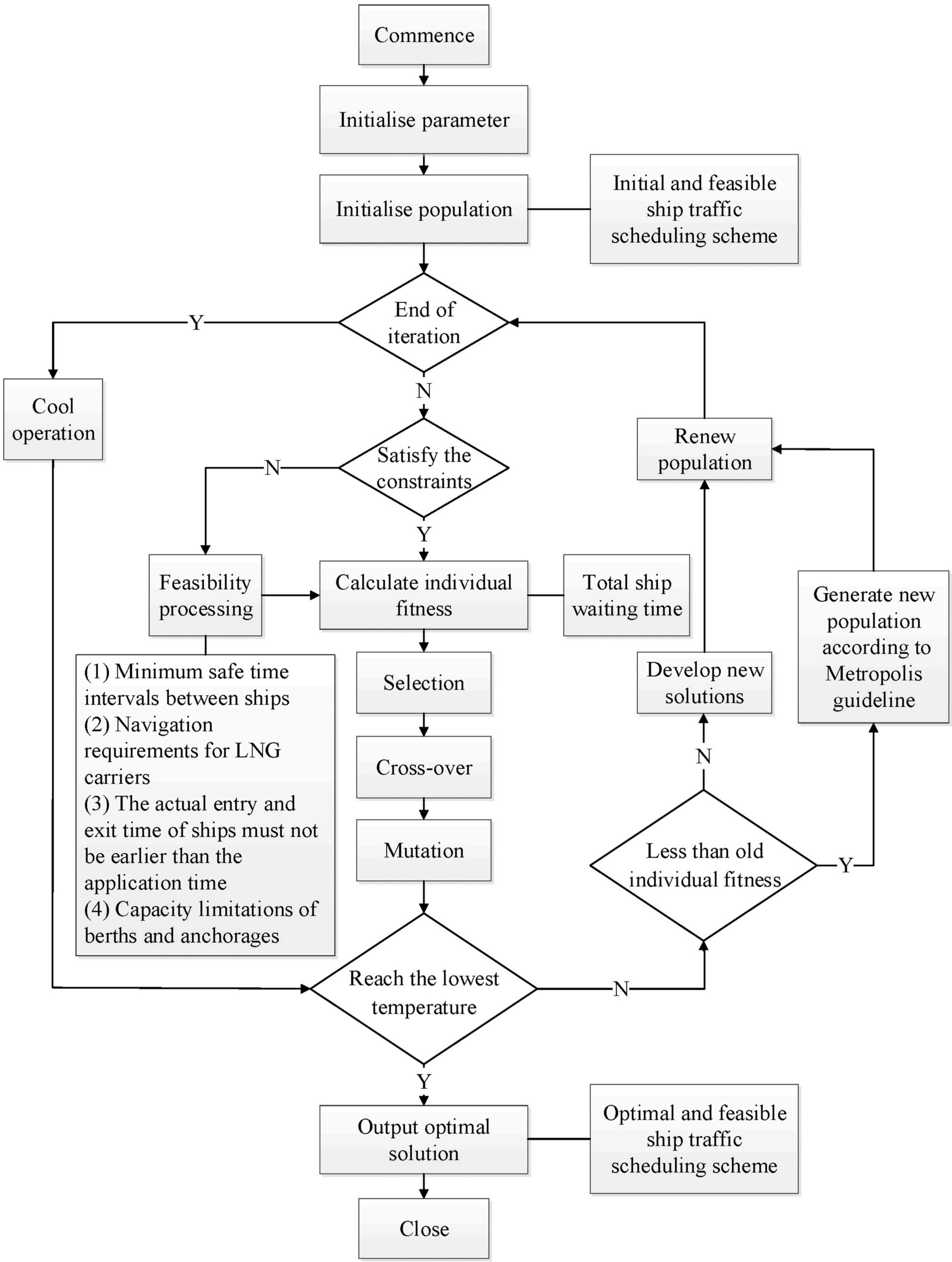

Fig. 3. Flowchart of improved simulated annealing genetic algorithm.

distance of the mobile safety zone from ships sailing in the same direction. These constraints are especially critical during LNG carrier night operations, as their mobile safety zones extend further, necessitating that no other ships enter their zone during nighttime, similar to what is required during the daytime. Constraints (9)–(12) and (27)–(28) imply that LNG carriers need to meet the requirements of navigation characteristics (mobile safety zone, one-way navigation) even during night navigation. Lastly, account for the unique risks associated with LNG carrier navigation at night, the minimum safe time interval for night-capable LNG carriers is set to be twice that of LNG carriers sailing during the daytime to ensure the safety of their night operations.

Finally, in order to reduce the complexity of the model and speed up the solution, a linearization process is performed on Constraint (8), and the result is as follows:

$$\psi(t) = t, 0 \leq t \leq \Upsilon \tag{33}$$

4. Algorithm design

Mixed-integer linear programming models can be solved using exact or approximate methods. For example, the branch and bound method and beam search algorithm can be implemented with programming using Gurobi, SCIP, etc. (Xiong et al., 2022). Alternatively, the constraint programming method can be employed with programming using CPLEX, Ortools, etc. (Liu et al., 2024b). Given that the port ship traffic scheduling problem is classified as NP-hard due to its complex model, a large number of variables, and multiple constraints, the time complexity associated with finding an exact solution is prohibitively high (Lalla-Ruiz et al., 2018). Due to the time-consuming nature of the exact algorithm, it is difficult to obtain a globally optimal solution even for small-scale arithmetic cases. Therefore, some scholars have proposed heuristic optimization methods to solve the port ship traffic scheduling problem, such as taboo search algorithm (Li et al., 2021b), genetic algorithm (Zhang et al., 2020), etc., which can obtain the relative optimal solution in a short time. Among them, genetic algorithms have favorable application prospects in port ship traffic scheduling (Nam and Lee, 2013; Tang et al., 2024). Compared with other optimization algorithms, the genetic algorithm utilizes the objective function value as search information and has a relatively simple process.

4.1. Genetic algorithm

The design process of a traditional genetic algorithm usually consists of five steps: selecting an appropriate encoding method, initializing the population, calculating the individual fitness, generating the next-generation population, and setting the termination iteration condition (Chen et al., 2023). Considering that the traditional genetic algorithm sets the crossover probability and mutation probability as constants, which may lead to premature convergence during the iteration process and a slow convergence rate when approaching the optimal solution, resulting in the algorithm obtaining a local optimal solution (Ning et al., 2023). This paper designs an adaptive adjustment mechanism to improve the crossover operator and mutation operator, and the implementation processes of their crossover and mutation probabilities are as follows:

$$P_c = \begin{cases} P_{c1} - \dfrac{(P_{c1} - P_{c2})(f_1 - f_{ave})}{f_{\max} - f_{ave}}, f_1 \geq f_{ave} \\ P_{c1}, f_1 < f_{ave} \end{cases} \tag{34}$$

$$P_m = \begin{cases} P_{m1} - \dfrac{(P_{m1} - P_{m2})(f_{\max} - f)}{f_{\max} - f_{ave}}, f \geq f_{ave} \\ P_{m1}, f < f_{ave} \end{cases} \tag{35}$$

Among them, f_1 represents the larger value of fitness among the two chromosomes after crossover, f_{ave} represents the mean value of the average fitness of the population, $f_{\max}$ represents the maximum fitness value in the population, P_{c1} is the maximum crossover probability, P_{c2} is the minimum crossover probability; f represents the individual fitness value, P_{m1} is the maximum mutation probability, P_{m2} is the minimum mutation probability, and $P_{c1} > P_{c2}$, $P_{m1} > P_{m2}$.

4.2. Improved simulated annealing genetic algorithm

To further enhance the solution quality and operational efficiency of the improved genetic algorithm, the annealing concept from the simulated annealing algorithm is incorporated. The salient advantage of the simulated annealing algorithm lies in its integration of the Metropolis criterion. This allows the algorithm to effectively break free from local optimal solutions and endows it with robust local search capabilities. In accordance with the Metropolis criterion, the probability of a particle attaining equilibrium at temperature T is given by $\exp(\Delta E/T)$, where E is the internal energy at temperature T and ΔE represents the change in internal energy. The annealing process is governed by a cooling schedule, which encompasses control parameters such as the initial value T_j, its attenuation factor K, the number of iterations I for each temperature value T, and the stopping condition. As a Monte Carlo sampling approach, the Metropolis concept stipulates that when an energy state within the system transitions to another, the energy shifts from E_1 to E_2. The formula for the transition probability is as follows:

$$\boldsymbol{p} = \exp\left(-\frac{E_1 - E_2}{T}\right) \tag{36}$$

When $E_2 < E_1$, the current latest state is accepted by the system. Otherwise, the latest state will be either accepted or rejected based on a random probability. The probability of state 2 being accepted is:

$$\boldsymbol{p} = \begin{cases} 1, E_2 < E_1 \\ \exp\left(-\dfrac{E_2 - E_1}{T}\right), E_2 \geq E_1 \end{cases} \tag{37}$$

The fitness values of the chromosomes of the new population generated through genetic operations are calculated. If the fitness value is greater than that of the corresponding chromosome in the old population, it is adopted as the new solution; if it is smaller, a new solution is generated according to the Metropolis criterion. A temperature reduction operation is performed on the new population to compensate for the relatively poor local optimization ability of the genetic algorithm and help the algorithm escape from local optimal solutions (Shen et al., 2024). Since the crossover and mutation parameters of GA remain fixed during the iterative search process, the search ability of the algorithm is relatively poor. In contrast, ISAGA can effectively avoid the destruction of excellent gene characteristics in the population and promote the generation of new individuals through an adaptive adjustment mechanism in each iteration, preventing the algorithm from falling into local optima and obtaining the global optimal total waiting time of ships. Therefore, this paper proposes to integrate the advantages of the adaptive adjustment mechanism and the simulated annealing algorithm into the conventional genetic algorithm. The improved genetic algorithm rapidly searches for the optimal or near-optimal solution in the solution space, and then the simulated annealing algorithm is used to search for a better solution based on this solution. The ISAGA algorithm incorporates an adaptive adjustment mechanism that effectively enhances search efficiency, addressing the complexities of ship traffic scheduling with LNG carrier-specific constraints. Traditional genetic algorithms often face the issue of premature convergence to local optima, limiting their ability to explore the solution space effectively. To mitigate this, ISAGA integrates simulated annealing and a dynamic cooling mechanism, which improves global search capability and enhances solution quality. These enhancements allow ISAGA to escape local optima, leading to more robust and accurate optimization results for ship traffic scheduling in LNG port areas.

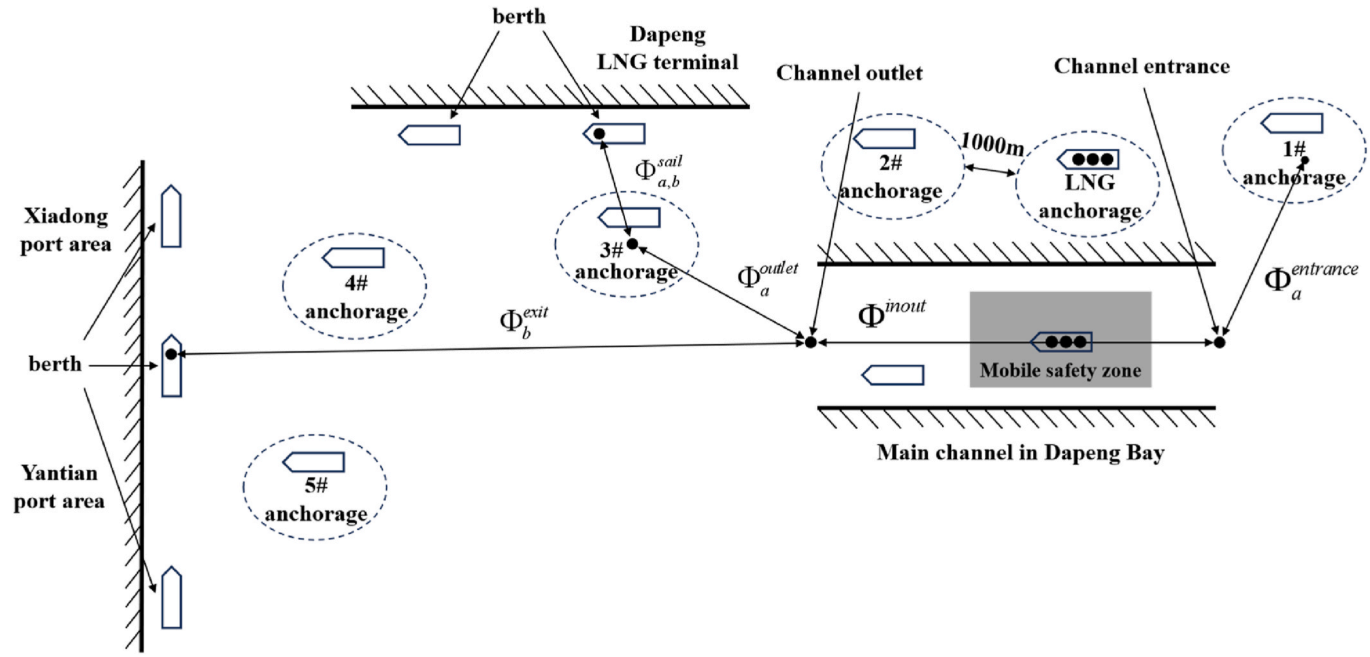

Fig. 4. Actual layout of Dapeng Bay port area in Shenzhen.

Table 1
Distance from each anchorage to the entrance or exit of the channel.

Anchorage number	Channel exit or entrance	Distance(n mile)
1#	Entrance	6.1
2#	Exit	3.8
3#	Exit	2.8
4#	Exit	3.3
5#	Exit	5.0
6#	Exit	4.5

The improved simulated annealing genetic algorithm is applied to solve the ship traffic scheduling problem in this paper, and the algorithm flowchart is shown in Fig. 3.

The main procedures of the improved simulated annealing genetic algorithm are as follows:

Step 1: Number the ships according to their quantity and the time sequence of their entry and exit applications. Take the time when ships apply for entry and exit as the lower limit and the set of planned periods during which ships can sail as the upper limit. Consider the ship number as the gene code. Sequentially and randomly generate the actual entry and exit times corresponding to the ship numbers and form a chromosome. Repeat this step to generate a specified number of chromosomes, thus form an initial population.

Step 2: Take the total waiting time of each ship as the fitness value. Calculate the fitness values of each chromosome in the population one by one.

Step 3: With the requirements of the safe time interval between ships sailing in the same direction, the one-way navigation requirement of LNG carriers, the requirement that the actual entry and exit time of ships is not earlier than the application time, and the requirement that the sailing time does not exceed the set of planned periods as the feasibility check mechanism, check each chromosome in the population. Eliminate the chromosomes that do not meet the requirements, regenerate new chromosomes and calculate their fitness values. Conduct a feasibility check on the new chromosomes until the required number of chromosomes in the population is met. In addition, each chromosome offspring needs to undergo a feasibility check. It is necessary to conduct four types of feasibility checks on the ship traffic scheduling scheme to determine whether crossover and mutation operations will lead to the generation of infeasible solutions: (1) The minimum safe time interval between ships sailing in the same direction. (2) One-way navigation, mobile safety zone and navigation time window of LNG carriers. (3) The actual entry and exit time of ships must not be earlier than the application time. (4) Capacity limitations of berths and anchorages.

Step 4: Based on the fitness values of individuals in the population, use the roulette wheel method to select individuals with small fitness values as parents to reproduce the next generation.

Step 5: For the selected parent individuals, randomly select the ship numbers and quantities in two chromosomes, perform crossover operations according to the improved crossover probability, and generate new offspring individuals.

Step 6: Perform mutation operations on the new offspring individuals with the improved mutation probability. Randomly select a certain number of ship numbers in the chromosome and regenerate the actual entry and exit times corresponding to these ship numbers according to the time upper and lower limit requirements.

Table 2
Distance from each berth to the channel exit.

Berth number	Distance(n mile)
1#-15#	6.9
16#-18#	6.9
19#-28#	4.2
29#	3.2
30#-31#	2.7

Table 3
Distance from each berth to inner anchorage.

Berth number	Anchorage number	Distance(n mile)
1#-15#	5#	2.7
16#-18#	2#	11.4
19#-28#	3#	1.8
16#-18#	4#	4.7
29#	6#	6.2
30#-31#	6#	6

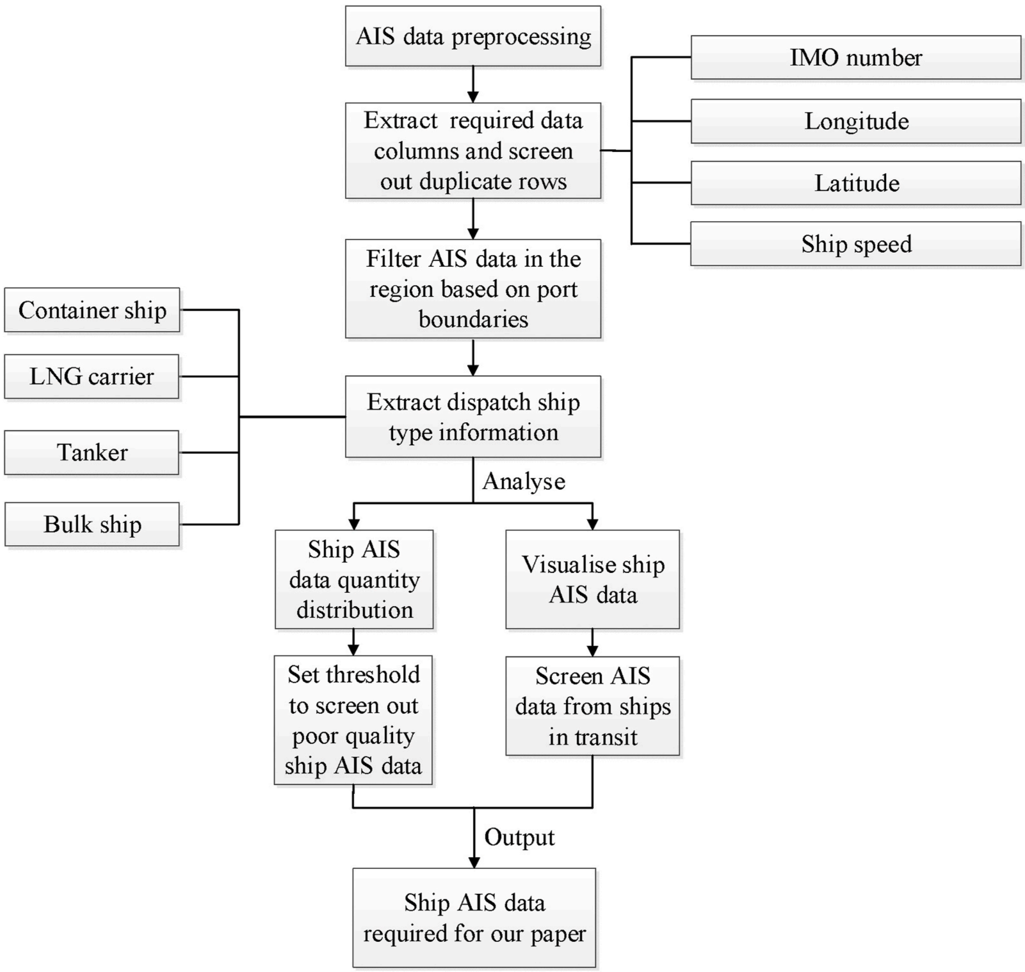

Fig. 5. AIS data preprocessing flowchart.

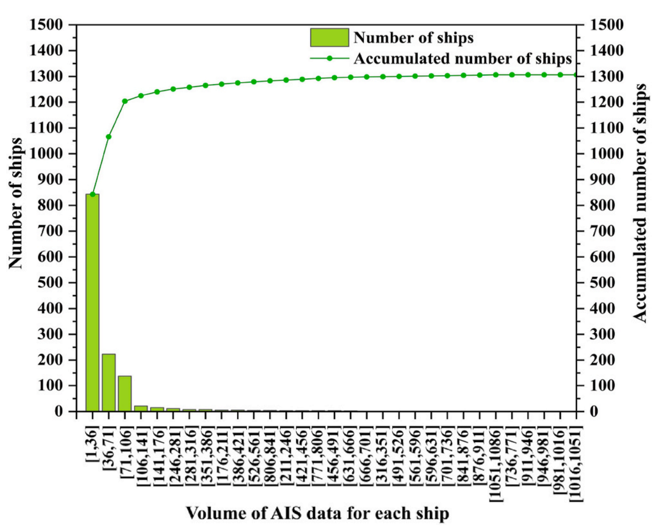

Fig. 6. Distribution of the number of ship AIS data.

Step 7: Combine the offspring individuals generated by crossover and mutation operations into a new population and conduct a feasibility check through Step 3.
Step 8: Calculate the fitness value of the offspring population. If this value is smaller than the fitness value of the old individual, a new solution is generated. If the value is larger than the fitness value of the old individual, a new solution is generated according to the Metropolis criterion.
Step 9: Perform a temperature reduction operation on the offspring population. If the minimum temperature is reached, the algorithm ends and outputs the individual with the smallest fitness value in the population at this temperature and the optimal ship traffic scheduling scheme. If the minimum temperature has not been reached, continue to return to Step 2 and loop the algorithm.

5. Numerical experiment

5.1. Basic information on port resources

The Shenzhen Dapeng Bay LNG hub port is the first large-scale LNG hub port in China. In the early stage of 2023, the number of ships entering and leaving the port area increased by 35.23 % compared with the same period last year, and the handling volume increased by 39.2 % compared with the same period last year, reaching a historical peak in LNG transportation (China Water Transportation Net, 2023). Based on the characteristics of the Shenzhen Dapeng Bay port area and the collected information of ship navigation trajectories, the following are determined:

(1) The set of all ship types $H = 4$, where $H = 1, 2, 3, 4$ represents container ships, LNG carriers, tankers, and bulk ships respectively. Considering the navigation characteristics of LNG carriers, set $\theta_{i,1}^{priority} = 0$, $\theta_{i,2}^{priority} = 1$, $\theta_{i,3}^{priority} = 0$, $\theta_{i,4}^{priority} = 0$, where $i \in$ E.

Table 4
Data of 76 ships.

Ship number	Inbound or Outbound	Ship type	Berth number	Anchorage number	Ship length (m)	Ship average speed (kn)	Minimum safe time interval (min)	Application start time (min)
1	Inbound	Container ship	1#	1#	347	12.9	15	0
2	Inbound	Container ship	2#	1#	304	13.4	15	24
3	Outbound	Container ship	1#	5#	222	12.4	15	46
4	Inbound	Container ship	3#	1#	367	12.1	15	97
5	Outbound	Container ship	2#	5#	267	14.5	15	121
6	Inbound	Container ship	4#	1#	366	12.4	15	178
7	Inbound	Container ship	5#	1#	366	14.1	15	213
8	Inbound	Container ship	6#	1#	400	11.7	15	249
9	Inbound	Container ship	7#	1#	366	10.2	15	288
10	Inbound	Container ship	8#	1#	249	13.6	15	324
11	Inbound	LNG carrier	29#	6#	288	5.5	40	369
12	Inbound	Container ship	9#	1#	398	8.7	15	415
13	Inbound	Container ship	10#	1#	300	12.8	15	476
14	Inbound	Container ship	11#	1#	300	10.1	15	523
15	Inbound	Container ship	1#	1#	300	15.9	15	574
16	Inbound	LNG carrier	30#	6#	290	12.3	20	613
17	Inbound	Container ship	2#	1#	400	11.3	15	682
18	Outbound	Container ship	3#	5#	400	13.1	15	746
19	Inbound	Bulk ship	16#	2#	135	7.9	10	798
20	Outbound	Container ship	4#	5#	400	11.7	15	915
21	Outbound	Container ship	5#	5#	366	13.8	15	978
22	Outbound	Container ship	6#	5#	400	12.7	15	1069
23	Outbound	Container ship	7#	5#	271	14.8	15	1124
24	Outbound	Container ship	8#	5#	172	12.3	10	1186
25	Outbound	Container ship	9#	5#	400	12.5	15	1247
26	Outbound	Container ship	10#	5#	186	13.4	10	1445
27	Inbound	Bulk ship	17#	2#	84	8.3	10	1513
28	Outbound	Container ship	11#	5#	347	14.6	15	1568
29	Inbound	Container ship	12#	1#	398	12.5	15	1637
30	Inbound	Container ship	13#	1#	271	14	15	1667
31	Inbound	Tanker	19#	3#	125	7.7	10	1716
32	Inbound	Container ship	14#	1#	304	13.3	15	1733
33	Inbound	Container ship	15#	1#	367	9.6	15	1767
34	Inbound	LNG carrier	31#	6#	292	4.4	40	1819
35	Inbound	Container ship	3#	1#	366	12.9	15	1882
36	Inbound	Container ship	4#	1#	366	12.7	15	1917
37	Inbound	Bulk ship	18#	2#	135	8.9	10	1996
38	Outbound	Container ship	1#	5#	366	13.1	15	2035
39	Outbound	Bulk ship	16#	4#	60	6.6	10	2097

(continued on next page)

Table 4 (*continued*)

Ship number	Inbound or Outbound	Ship type	Berth number	Anchorage number	Ship length (m)	Ship average speed (kn)	Minimum safe time interval (min)	Application start time (min)
40	Inbound	Container ship	5#	1#	300	8.2	15	2158
41	Outbound	Bulk ship	17#	4#	75	7.4	10	2243
42	Outbound	Container ship	12#	5#	400	11.2	15	2344
43	Outbound	Container ship	13#	5#	400	14.1	15	2369
44	Outbound	Container ship	14#	5#	366	13.9	15	2408
45	Outbound	LNG carrier	30#	6#	288	4.2	40	2469
46	Outbound	Tanker	19#	3#	122	7.1	10	2521
47	Outbound	Container ship	2#	5#	365	11.9	15	2569
48	Inbound	Container ship	1#	1#	172	12.4	10	2622
49	Outbound	Container ship	15#	5#	400	13	15	2696
50	Outbound	Bulk ship	18#	4#	84	8.7	10	2728
51	Inbound	Bulk ship	16#	2#	84	7.9	10	2797
52	Outbound	Container ship	3#	5#	184	11	10	2895
53	Outbound	Container ship	4#	5#	277	14.2	15	2949
54	Outbound	Container ship	5#	5#	347	13.6	15	2995
55	Outbound	Container ship	1#	5#	304	12.9	15	3043
56	Inbound	Container ship	6#	5#	367	13.1	15	3097
57	Inbound	Container ship	7#	1#	366	13.3	15	3144
58	Inbound	Container ship	8#	1#	366	12.2	15	3195
59	Inbound	Container ship	9#	1#	366	14	15	3234
60	Inbound	Container ship	10#	1#	366	15.3	15	3289
61	Inbound	Container ship	11#	1#	399	13.8	15	3323
62	Inbound	LNG carrier	30#	6#	288	11.5	20	3378
63	Inbound	Container ship	12#	1#	398	12.9	15	3426
64	Inbound	Container ship	13#	1#	300	12.3	15	3467
65	Outbound	Bulk ship	16#	4#	135	9.3	10	3498
66	Inbound	Container ship	14#	1#	400	16.7	15	3535
67	Inbound	Container ship	15#	1#	400	11.8	15	3579
68	Outbound	Container ship	6#	5#	322	13.6	15	3623
69	Inbound	Bulk ship	17#	2#	79	8	10	3657
70	Inbound	Bulk ship	18#	2#	80	7.3	10	3699
71	Inbound	Tanker	20#	3#	125	6.4	10	3745
72	Outbound	Container ship	7#	5#	365	12.9	15	3856
73	Outbound	Container ship	8#	5#	366	10.7	15	3901
74	Outbound	Bulk ship	17#	4#	84	9	10	3986
75	Inbound	Container ship	2#	1#	366	13.9	15	4067
76	Outbound	Tanker	20#	3#	138	6.9	10	4122

(2) The maximum number of ships that can wait at each anchorage $\Gamma_1^{max} = 50, \Gamma_2^{max} = 7, \Gamma_3^{max} = 8, \Gamma_4^{max} = 15, \Gamma_5^{max} = 6, \Gamma_6^{max} = 3$, and the set of anchorages $A = 6$. The set of berths $B = 31$

(3) The number of berths for type h ships in the port $\delta_1 = 15, \delta_2 = 3, \delta_3 = 10, \delta_4 = 3$. The planned number of days is 3, that is, $n = 3$. At the start of the planned period, the number of type h ships already berthed at the port $\delta_1^{begin} = 0$, $\delta_2^{begin} = 0$, $\delta_3^{begin} = 0$, $\delta_4^{begin} = 0$.

This study is based on the layout of the Shenzhen Dapeng Bay port area, as shown in Fig. 4. The Shenzhen Dapeng Bay waters possess a two-way main channel with a total length of 7.4 nautical miles, a total of 6 inner and outer anchorages, and 31 berths. Anchorages 2# - 6# are inner anchorages, among which 6# is a dedicated LNG anchorage and 1# is an outer anchorage. Berths 1# - 15# are container berths in the Yantian port area. Berths 16# - 18# are bulk and general cargo berths in the Yantian port area. Berths 19–28# are hazardous cargo berths for oil

Table 5
Optimal traffic organization scheme for 76 ships.

Ship number	Inbound or Outbound	Berth number	Application start time (min)	Actual start time(min)	FCFS actual start time(min)	Time to enter the channel (min)	Time to leave the channel (min)	Arrival time of anchorage(min)	Arrival time of berth(min)
1	1	1#	0	0	97	29	64	/	97
4	1	3#	97	139	297	139	176	/	211
2	1	2#	24	173	188	201	235	/	266
3	0	1#	46	216	249	241	277	60	/
7	1	5#	213	238	487	264	296	/	326
8	1	6#	249	253	548	253	291	/	327
9	1	7#	288	302	633	302	346	/	387
11	**1**	**29#**	**369**	**427**	**730**	**427**	**508**	/	**543**
6	1	4#	178	513	396	543	579	/	613
12	**1**	**9#**	**415**	**563**	**781**	**606**	**658**	/	**706**
13	1	10#	476	609	803	638	673	/	706
10	1	8#	324	628	689	655	688	/	719
16	**1**	**30#**	**613**	**669**	**903**	**669**	**706**	/	**718**
5	0	2#	121	719	358	740	771	133	/
14	1	11#	523	803	823	803	847	/	888
18	0	3#	746	813	987	836	870	759	/
15	1	1#	574	908	859	932	960	/	987
20	0	4#	915	1103	1097	1129	1167	929	/
19	1	16#	798	1126	1064	798	855	884	1213
21	0	5#	978	1148	1186	1170	1203	990	/
23	0	7#	1124	1168	1327	1189	1219	1135	/
24	0	8#	1186	1199	1364	1233	1270	/	/
17	1	2#	682	1248	946	1281	1321	/	1358
25	0	9#	1247	1314	1484	1338	1374	1260	/
22	0	6#	1069	1335	1288	1359	1394	1082	/
30	1	13#	1667	1671	1867	1698	1730	/	1760
32	1	14#	1733	1828	1994	1828	1862	/	1894
29	1	12#	1637	1843	1759	1843	1879	/	1913
31	1	19#	1716	1858	1946	1716	1774	1796	1873
34	**1**	**31#**	**1819**	**1898**	**2089**	**1898**	**1999**	/	**2036**
27	1	17#	1513	1994	1647	1513	1567	1595	2077
37	1	18#	1996	2012	2288	2012	2062	/	2109
26	0	10#	1445	2063	1608	2086	2120	1458	/
35	1	3#	1882	2088	2186	2117	2152	/	2185
28	0	11#	1568	2135	1698	2156	2187	1580	/
36	1	4#	1917	2173	2234	2202	2237	/	2270
33	1	15#	1767	2224	2048	2224	2271	/	2315
41	0	17#	2243	2306	2496	2362	2422	/	/
39	0	16#	2097	2348	2387	2378	2446	2140	/
43	0	13#	2369	2433	2579	2455	2487	2381	/
38	0	1#	2035	2468	2346	2491	2525	2048	/
45	**0**	**30#**	**2469**	**2508**	**2673**	**2547**	**2653**	/	/
42	0	12#	2344	2636	2526	2663	2703	2359	/
46	0	19#	2521	2651	2718	2675	2738	2537	/
40	1	5#	2158	2653	2442	2698	2753	/	2804
47	0	2#	2569	2692	2743	2718	2756	2583	/
44	0	14#	2408	2718	2621	2740	2772	2420	/
48	1	1#	2622	2720	2776	2750	2786	/	2820
50	0	18#	2728	2765	2820	2813	2865	/	/
49	0	15#	2696	2840	2798	2864	2899	2709	/
51	1	16#	2797	2867	2866	2867	2924	/	2977
52	0	3#	2895	2992	2945	3020	3061	2910	/
54	0	5#	2995	3021	3149	3052	3085	/	/
53	0	4#	2949	3188	3086	3210	3242	2961	/
56	1	6#	3097	3219	3299	3219	3253	/	3285
57	1	7#	3144	3242	3343	3270	3304	/	3336
55	0	1#	3043	3253	3246	3277	3312	3056	/
58	1	8#	3195	3257	3388	3287	3324	/	3358
60	1	10#	3289	3299	3498	3323	3353	/	3381
62	**1**	**30#**	**3378**	**3378**	**3596**	**3378**	**3417**	/	**3432**
61	1	11#	3323	3453	3542	3480	3513	/	3543
59	1	9#	3234	3494	3446	3521	3553	/	3583
65	0	16#	3498	3517	3759	3562	3610	/	/
64	1	13#	3467	3589	3686	3619	3656	/	3690
67	1	15#	3579	3634	3845	3666	3704	/	3740
68	0	6#	3623	3687	3897	3710	3743	3635	/
66	1	14#	3535	3771	3806	3771	3798	/	3823
63	1	12#	3426	3786	3645	3786	3821	/	3854
71	1	20#	3745	3801	4065	3801	3871	/	3911
72	0	7#	3856	3893	4097	3917	3952	3869	/
69	1	17#	3657	3974	3947	3657	3713	3742	4060
73	0	8#	3901	4050	4158	4079	4121	3917	/

(*continued on next page*)

Table 5 (*continued*)

Ship number	Inbound or Outbound	Berth number	Application start time (min)	Actual start time(min)	FCFS actual start time(min)	Time to enter the channel (min)	Time to leave the channel (min)	Arrival time of anchorage(min)	Arrival time of berth(min)
75	1	2#	4067	4092	4267	4092	4124	/	4154
70	1	18#	3699	4117	3994	3699	3760	3792	4211
74	0	17#	3986	4175	4231	4197	4247	4018	/
76	0	20#	4122	4242	4305	4267	4332	2138	/

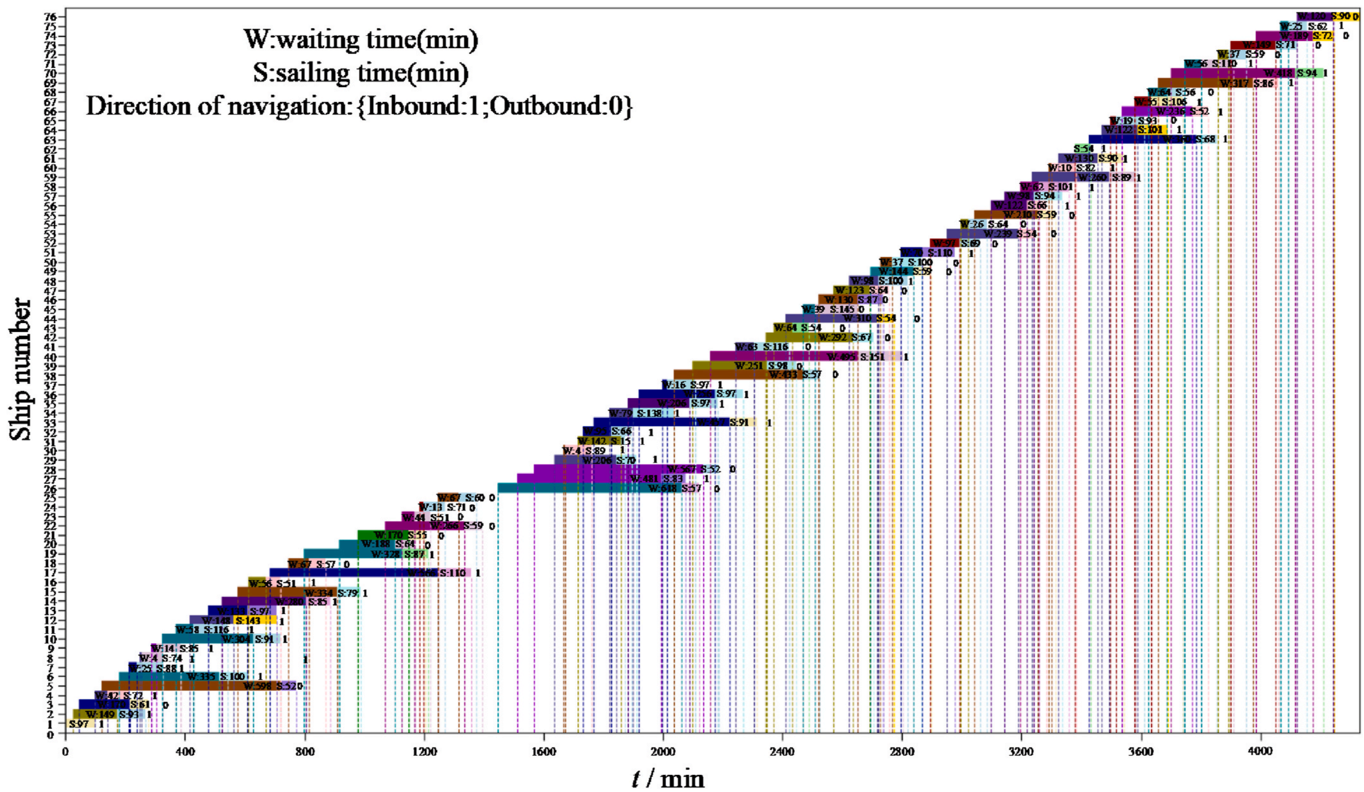

Fig. 7. Gantt chart of optimal scheduling scheme for 76 ships.

and gas in the Xiadong port area. Berth 29# is an LNG berth at the China National Petroleum Corporation LNG terminal. Berths 30# - 31# are LNG berths at the Dapeng LNG terminal. In Fig. 4, in order to ensure that the LNG carrier always maintains a safe distance from other ships in the same direction when navigating and to prevent other ships from affecting the navigation safety of the LNG carrier, as well as to disallow

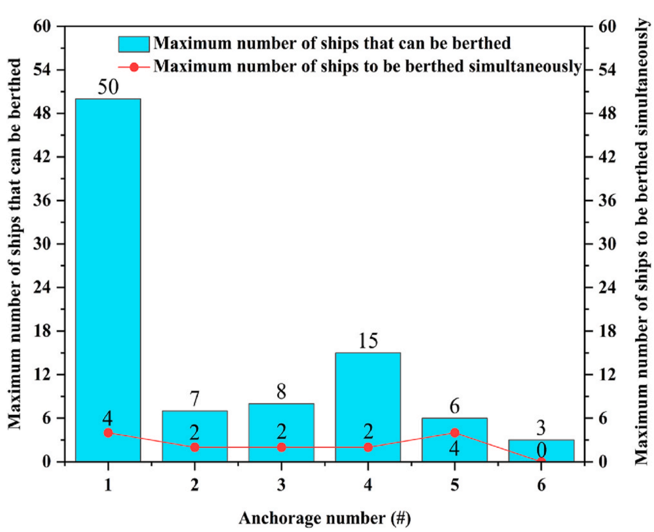

Fig. 8. Plot of the maximum results of the actual number of ships simultaneously at anchor at each anchorage during the planning period.

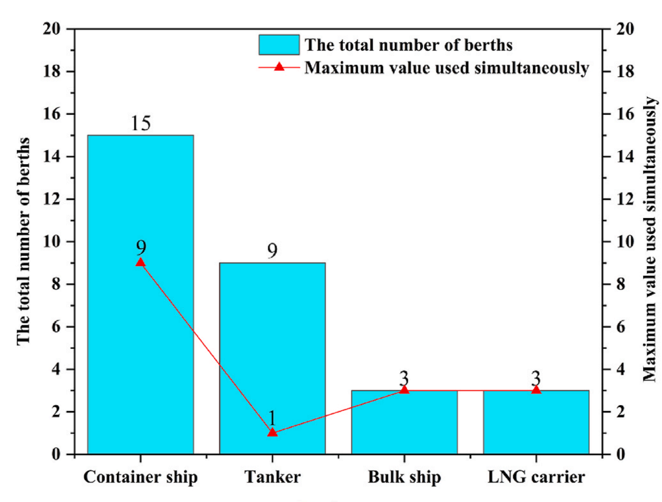

Fig. 9. Plot of the maximum value of the actual number of all types of berths used simultaneously in the planning period.

the navigation of ships in the opposite direction, the LNG carrier has been provided with a mobile safety zone, and no other ships are allowed to enter the mobile safety zone of the LNG carrier. For the convenience of calculation, the distance from the topographic center of each anchorage to the entrance and exit of the channel is taken as the measurement, and the specific results are shown in Table 1. Similarly, the distances between each berth and the exit of the channel are shown in Table 2, and the distances between each berth and the inner anchorages are shown in Table 3.

5.2. Data collection and processing

Considering the impact of the navigation characteristics of LNG carriers on the ship traffic scheduling in the Dapeng Bay port area, the navigation trajectory data of all ships, including LNG carriers, in three consecutive days in December 2023 in the Shenzhen Dapeng Bay port area were collected and preprocessed. The data preprocessing flowchart is shown in Fig. 5.

To obtain clean and reliable Automatic Identification System (AIS) data for the experimental analysis part of this paper, it is necessary to conduct comprehensive data processing on the AIS data. We first extract the IMO number, ship latitude and longitude, and ship speed information from the AIS data of December 2023, and delete the duplicate data rows. Secondly, we eliminate the AIS data outside the port area based on the spatio-temporal range of the port. Accordingly, 858,677 AIS data are screened out, leaving 189,898 AIS data. We then clean the ship type data by eliminating irrelevant ship type data such as fishing boats and yachts, as well as abnormal characteristic data of ships with a length less than 10 m or without length information. The remaining ship types are container ships, LNG carriers, tankers, and bulk ships. 3430 ship type data are deleted, leaving 3895 ship type data. Then, we perform the association processing between the cleaned ship type data and the AIS data. 122,114 AIS data and 2589 ship type data are screened out, leaving 67,784 AIS data and 1306 ship type data. Fig. 6 shows the distribution of the quantity of ship AIS data. To effectively screen out the AIS data of ships with poor quality and in transit, we set the threshold that the quantity of ship AIS data is not greater than 45. A total of 39,136 AIS data and 1012 ship type data are screened out, leaving 28,648 AIS data and 294 ship type data.

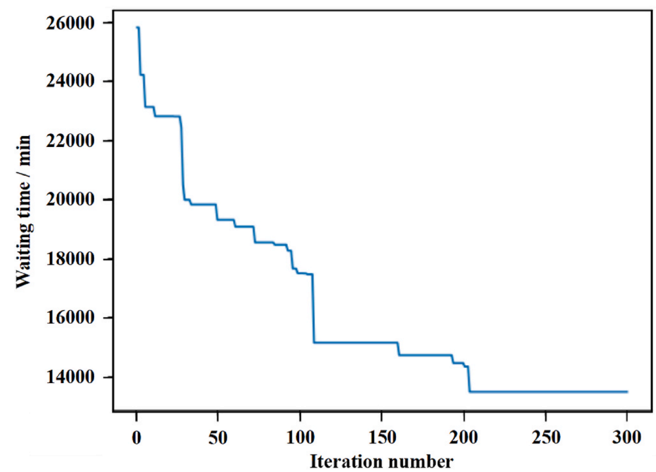

Fig. 11. Convergence curve of ISAGA.

After the data preprocessing, the remaining ship AIS data are associated with the ship type data. Finally, we obtained the visit volumes of various types of ships in the Dapeng Bay port area in December 2023 as follows: 256 container ships, 18 LNG carriers, 10 tankers, and 10 bulk ships. The processed ship-related data are shown in Table 4. This data includes ship numbers, entry and exit directions, berth numbers where ships dock, anchorage numbers where ships anchor, average ship speeds, and times when ships apply for entry and exit.

Using Shenzhen Dapeng Bay port area as an example, we constructed an instance calculation of the mixed-integer linear programming model. To further verify the effectiveness of the model, this paper designs comparative experiments with different scales of ship visit volumes. The experiments were conducted on a computer equipped with an Inter(R) Core(TM) i7-12700H CPU @ 2.30 GHz processor and 32 GB of RAM, utilizing example programs within the Python framework PyCharm version 2023.

Table 5 presents the optimal traffic organization scheme for 76 ships obtained by the proposed model. For instance, the 10th ship to be scheduled is the inbound ship numbered 12. The starting scheduling

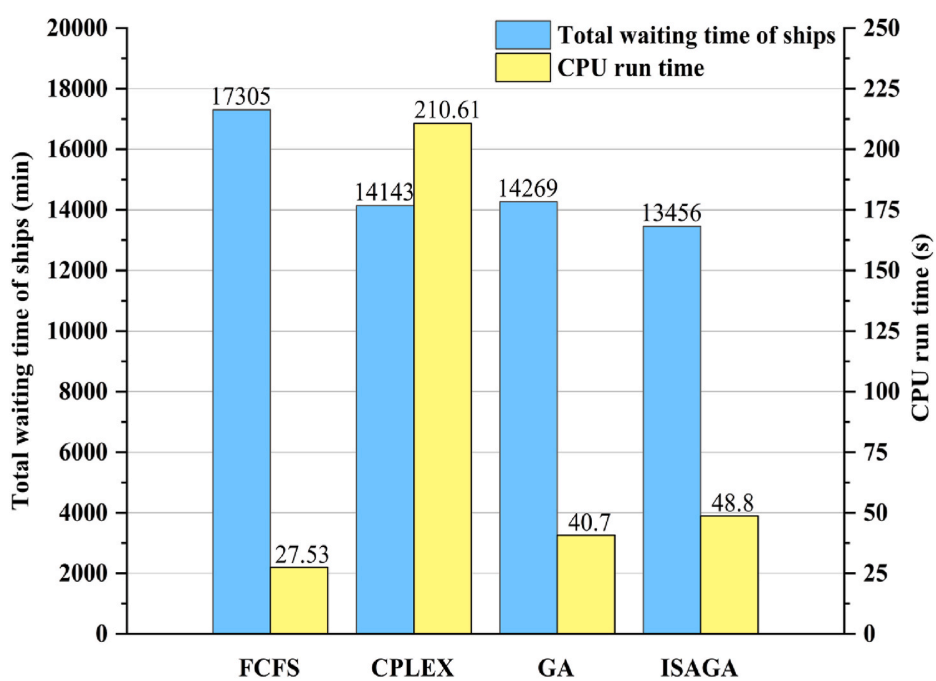

Fig. 10. Comparison between the results of FCFS, CPLEX, GA, and ISAGA.

Table 6
Comparison of results in cases with different total number of ships and LNG carriers.

Total number of ships	Number of LNG carriers	Total waiting time of ISAGA (min)	Total waiting time of FCFS (min)	Planning cycle ϒ (min)
25	0	2995	4087	1440
25	1	3076	4155	1440
25	3	3215	4273	1440
25	5	3428	4419	1440
50	0	8041	11058	2880
50	1	8159	11124	2880
50	3	8417	11297	2880
50	5	8663	11533	2880
75	0	11735	16499	4320
75	1	11914	16672	4320
75	3	12383	16825	4320
75	5	12854	17114	4320

time is 563 min, the time of entering the waterway is 606 min, the time of leaving the waterway is 658 min, and the time of arriving at the berth is 706 min. Fig. 7 further shows the optimal scheduling scheme for 76 ships. The figure not only provides a clear visualization of the optimal ship traffic organization scheme and the inbound or outbound directions for the 76 ships, but also effectively displays the waiting times and sailing times for each individual ship.

5.3. Verification of model validity

Fig. 8 shows that, within the planning period, the maximum number of ships waiting at anchorages during peak times is 4, which does not reach the upper limit of the number of ships that can wait at each anchorage. Among them, the maximum number of ships that can wait at the 6# LNG anchorage is 3, but the actual number of ships waiting during peak times is 0. This indicates that LNG carriers can navigate normally within the planning period, and the existing anchorage resources can accommodate a larger number of LNG carriers. The maximum actual concurrent usage numbers of various types of berths within the planning period are shown in Fig. 9. The concurrent usage numbers of berths for bulk ships and LNG carriers have reached the upper limit, while those for container ships and tankers have not. The concurrent usage number of tanker berths is only 1, and 8 tanker berth resources are idle. This shows that there is an imbalance in the utilization of existing berth resources of different types. Through the results of Figs. 8 and 9, it can be found that the concurrent usage number of LNG carrier berths has reached the upper limit, but the number of ships waiting at the 6# LNG anchorage during peak times is still 0. This illustrates that the scheduling strategy of LNG carriers in this paper's model makes full use of the existing LNG carrier berth resources. The above analysis indicates that the solution results meet the requirements of port resource usage limitations, demonstrating the effectiveness of the model's resource constraints.

Table 7
Comparison of results in cases with different total number of ships and night-capable LNG carriers.

Total number of ships	Number of LNG carriers	Total waiting time of ISAGA (min)	Total waiting time of FCFS (min)	Planning cycle ϒ (min)
25	0	2995	4087	1440
25	1	3183	4326	1440
25	3	3414	4519	1440
25	5	3659	4776	1440
50	0	8041	11058	2880
50	1	8329	11339	2880
50	3	8706	11645	2880
50	5	9114	12073	2880
75	0	11735	16499	4320
75	1	12173	16882	4320
75	3	12757	17258	4320
75	5	13496	17756	4320

5.4. Verification of model rationality

The rationality of the model can be analyzed from constraints such as navigation continuity, navigation rules of LNG carriers, and sailing time intervals between ships in the same direction. From the results of the optimal scheduling scheme in Tables 5 and it can be known that the order of ships entering and leaving the port and the navigation continuity of each ship are maintained, and a safe time interval is always kept between two ships sailing in the same direction. For example, for the outbound ships numbered 21 and 23, which are the 20th and 21st ships to be scheduled, the time differences in their arrival at the anchorage, starting scheduling time, time of entering the waterway, and time of leaving the waterway are 145 min, 20 min, 19 min, and 16 min respectively, all meeting the requirement that the minimum safe time interval for two outbound container ships is 15 min. In addition, the start and end scheduling times of the inbound LNG carriers numbered 16 and 62 are within the daytime time intervals of LNG carriers [480 min, 1080 min] and [3360 min, 3960 min].

During the scheduling process of LNG carriers, there is always no opposite-direction ship sailing. For the inbound LNG carrier numbered 11, which is the 8th ship to be scheduled, its starting scheduling time is 427 min and the time of arriving at the berth is 543 min. There is no outbound ship scheduled for operation within the time window of [427 min, 543 min].

Under the condition that LNG carriers are allowed to sail at night, the application time for the inbound LNG carrier numbered 34 to enter the port is 1819 min, while the actual time of entry is 1898 min. In comparison, the First-Come-First-Served (FCFS) method results in an entry time of 2089 min. Both the proposed method and the FCFS method meet the constraint that the actual entry time is not earlier than the requested application time. However, the proposed method reduces the waiting time outside the port by 191 min by prioritizing LNG carrier scheduling. This not only enhances scheduling efficiency but also reduces the navigational risk for LNG carriers, taking into account the additional requirements for escorting and lighting during nighttime voyages. Through analysis, it can be concluded that the results of the optimal scheduling scheme obtained in this paper are consistent with the navigation rules of ships in the same direction and the navigation rules of LNG carriers, indicating that the constraints in terms of the navigation rules of LNG carriers and the navigation rules of ships in the same direction are reasonable.

Table 8
Comparison of the results of the total waiting time for LNG carriers for different total number of ships with LNG carriers or night-capable LNG carriers.

Total number of ships	Number of LNG carriers	Total waiting time for LNG carriers (min)	Number of night-capable LNG carriers	Total waiting time for night-capable LNG carriers (min)	Planning cycle ϒ (min)
25	1	34	1	41	1440
25	3	138	3	145	1440
25	5	222	5	213	1440
50	1	47	1	42	2880
50	3	1046	3	239	2880
50	5	1215	5	326	2880
75	1	79	1	75	4320
75	3	1178	3	273	4320
75	5	1935	5	419	4320

Table 9
Comparison of results for maximum LNG berth occupancy value in cases with different total number of ships with LNG carriers or night-capable LNG carriers.

Total number of ships	Number of LNG carriers	Maximum value used simultaneously	Number of night-capable LNG carriers	Maximum value used simultaneously	Planning cycle Υ (min)
25	0	0	0	0	1440
25	1	1	1	1	1440
25	3	2	3	2	1440
25	5	3	5	3	1440
50	0	0	0	0	2880
50	1	1	1	1	2880
50	3	2	3	2	2880
50	5	3	5	2	2880
75	0	0	0	0	4320
75	1	1	1	1	4320
75	3	2	3	1	4320
75	5	3	5	2	4320

5.5. Comparison between FCFS, CPLEX, GA, and ISAGA

In this paper, three methods, namely CPLEX, GA, and ISAGA, are employed to solve the established model and compared with the results obtained by the FCFS method. We evaluate the performance of ISAGA in comparison with the other three methods in terms of both the objective value and CPU running time. The parameter values of ISAGA are as follows: maximum number of evolutionary generations $G = 300$, population size $N = 20$, maximum crossover probability $P_{c1} = 0.8$, minimum crossover probability $P_{c2} = 0.7$, maximum mutation probability $P_{m1} = 0.1$, minimum mutation probability $P_{m2} = 0.01$, initial temperature $T_{\max} = 100$, termination temperature $T_{\min} = 0.001$, attenuation coefficient $\xi = 0.98$. Currently, the FCFS method is frequently used in port ship traffic scheduling, which schedules ships in the order of their application scheduling times. The calculation results and CPU running times of FCFS, CPLEX, GA, and ISAGA are shown in Fig. 10. As shown in Fig. 10, although the CPU running time of ISAGA is not significantly lower than that of the Genetic Algorithm (GA), this may be due to the problem scale being suitable for heuristic optimization. However, ISAGA produces significantly better solution results than GA, demonstrating its superior optimization capability. Compared to CPLEX, ISAGA not only achieves better performance in terms of computational efficiency but also reduces the objective value by 687 min, highlighting its effectiveness in minimizing ship waiting times. Moreover, ISAGA outperforms both CPLEX and GA by delivering more effective ship traffic scheduling solutions in a shorter time, offering valuable decision support for port managers in optimizing resource allocation and improving overall port scheduling efficiency. As illustrated in Fig. 11, ISAGA stabilizes around the 200th iteration after 300 generations of calculation, achieving a minimum total waiting time of 13,456 min for scheduling 76 ships. Compared to the first-come-first-served (FCFS) method, ISAGA reduces the total waiting time by 3849 min, resulting in a 22.24 % improvement in scheduling efficiency, further demonstrating the superiority of the proposed model.

Table 10
Maximum number of ships with different total number of ships for LNG carriers or night-capable LNG carriers with normal voyage.

Total number of ships	Maximum number of LNG carriers	Maximum number of night-capable LNG carriers	Planning cycle Υ (min)
25	8	9	1440
50	12	16	2880
75	15	23	4320

Clarification:non-normal voyage means that the berths for LNG carriers are fully occupied and the number of ships waiting in the LNG anchorage has reached the maximum number of ships, and the LNG carriers need to wait outside the port.

6. Result analysis

6.1. Robustness analysis

In this subsection, the robustness of the model proposed in this paper is analyzed. Computational examples are carried out to verify different scales of ship visit volumes and the growth of LNG carrier visit volumes, and the solution results are shown in Table 6. Considering the LNG carrier arrival data from Shenzhen Dapeng Bay port area for three consecutive days in December 2023, the average number of LNG carriers arriving per day was between 1 and 2, with a total of 5 LNG carriers recorded during this period. Additionally, the total number of ships entering and leaving the port during this time was 76, which means that, on average, 25 ships entered and exited the port each day. Based on this data, we have selected three experimental periods corresponding to 1 day (1440 min), 2 days (2880 min), and 3 days (4320 min). Accordingly, the number of LNG carriers considered in the analysis was set to 0, 1, 3, and 5, while the total number of ships entering and exiting the port during these periods was set to 25, 50, and 75, respectively. To ensure consistency in the sensitivity and impact analyses, we assumed uniform routes, speeds, and navigation characteristics for all ships of the same type. This assumption was made to eliminate potential discrepancies caused by differences in navigation performance between ships, which could otherwise skew the analysis results. In addition, the average value of 15 calculation results is used for comparative analysis to account for accidental errors.

Analysis of the results in Table 6 shows that under the condition of the same ship visit volume E and planned period Υ, as the visit volume of LNG carriers in the experimental examples increases, the minimum total waiting time of ships for both the constructed model and the FCFS method increases significantly. This indicates that the navigation of LNG carriers has a major impact on the efficiency of ship traffic scheduling.

6.2. Impact analysis of LNG carrier opening night navigation

To investigate the impact of changes in the visit volume of LNG carriers after night navigation opening on the efficiency of ship traffic scheduling, a computational example analysis was conducted on the total visit volume of different scales of ships and the visit volume of night-capable LNG carriers. The solution results are shown in Table 7. It can be seen from Table 7 that when the ship visit volume E and the planned period Υ are fixed, as the number of LNG carriers that can navigate at night increases, the optimal solutions obtained by the ISAGA and FCFS methods also increase gradually, further demonstrating that the navigation of LNG carriers has a significant impact on the efficiency of ship traffic scheduling.

It can be observed from the results in Tables 6 and 7 that considering different total visit volumes of ships, visit volumes of LNG carriers, and visit volumes of night-capable LNG carriers, the objective values of

ISAGA are all better than the FCFS method commonly used in ports. For example, in Table 6, when the total number of ship visits increases from 25 to 75 and the number of LNG carrier visits increases from 1 to 5, both of the methods in this paper can improve the efficiency of port ship scheduling by more than 20 % compared to the FCFS method. Moreover, when the total visit volume of ships and the visit volume of LNG carriers are fixed, the opening of night navigation for LNG carriers will lead to a certain increase in the total waiting time of ships, but the increase range is relatively small.

To further analyze the impact of the visit volume of LNG carriers on the overall ship traffic scheduling efficiency in the port area, considering the cases of different visit volumes of LNG carriers and visit volumes of LNG carriers that can navigate at night, the calculation results are shown in Table 8. It can be seen from Table 8 that under the condition of a certain visit volume of LNG carriers, as the total visit volume of ships and the planned period increase, the total waiting time of LNG carriers that can navigate at night is significantly less than that of LNG carriers. For example, when the visit volume of LNG carriers is 3, the total visit volume of ships is 50 and 75, and the planned period is 2880 min and 4320 min respectively, the total waiting time of LNG carriers after the opening of night navigation is reduced by 807 min and 905 min respectively. Therefore, the opening of night navigation for LNG carriers effectively reduces the waiting time of LNG carriers in the port and improves the scheduling efficiency of LNG carriers. This conclusion provides a certain reference basis for port managers when making decisions on whether to open night navigation for LNG carriers.

6.3. *Sensitivity analysis*

In this section, computational example experiments with different scales of ship visit volumes were designed to conduct a sensitivity analysis of the model from two aspects: the utilization of LNG berths during peak periods and the maximum number of LNG carriers that can navigate normally. The utilization of LNG berths during peak periods under different total visit volumes of ships and different visit volumes of LNG carriers is shown in Table 9. It can be seen from Table 9 that under the condition of fixed total visit volumes of ships and visit volumes of LNG carriers, the opening of night navigation for LNG carriers can make more berth resources available, allowing more LNG carriers to enter and leave the port, thereby enhancing the utilization efficiency of port berth resources. For example, when the total visit volumes of ships are 50 and 75 respectively and the visit volumes of LNG carriers are both 5, the number of occupied LNG berths during peak periods of LNG carriers is 3, which has reached the upper limit of the existing number of LNG berths in the port. However, after the opening of night navigation for LNG carriers, the number of occupied LNG berths during peak periods is 2, effectively releasing one LNG berth resource for utilization.

Under the existing port resource conditions, to explore the number of LNG carriers that can navigate in the port before and after the opening of night navigation for LNG carriers, a comparative experiment under different total visit volumes of ships and planned periods was designed, and the calculation results are shown in Table 10. Through the analysis of Table 10 and it can be concluded that when the total visit volume of ships and the planned period are fixed, the opening of night navigation for LNG carriers enables the port to accommodate a larger number of LNG carriers. When the total visit volumes of ships in Table 10 are 25, 50, and 75 respectively, the maximum number of normal navigations of LNG carriers after the opening of night navigation is increased by 1, 4, and 8 respectively compared with that before the opening. The results show that the opening of night navigation for LNG carriers effectively improves the ability of LNG carriers to visit the port and also indicates that port resources such as LNG berths and anchorages are efficiently utilized. This conclusion can provide a good reference for accommodating a larger number of LNG carriers in the port waters and improving the efficiency of ship traffic scheduling.

7. Conclusion

This paper investigates the ship traffic scheduling problem in LNG port areas, incorporating the navigation characteristics of LNG carriers—such as one-way navigation, mobile safety zones, and navigation time windows—and the risks associated with night navigation. A MILP model is developed to minimize the total waiting time of ships entering and leaving the port. To solve this complex problem, an ISAGA-based approach is proposed, yielding optimal ship sequencing and traffic scheduling schemes. Using Shenzhen Dapeng Bay as a case study, the model's applicability is validated with real-world data from 76 ships, accounting for the port's physical layout and navigation rules. The results demonstrate that the proposed optimization model significantly outperforms the FCFS method, verifying the model's rationality, effectiveness, and superior optimization performance. Comparisons with CPLEX and a standard genetic algorithm further confirm the robustness and computational efficiency of ISAGA.

A robustness analysis examines the model's performance under varying ship visit volumes, LNG carrier visit volumes, and the inclusion of night navigation. The findings highlight the model's scalability and adaptability, showing substantial reductions in total waiting times compared to the traditional FCFS method, particularly as ship visit volumes increase. Additionally, enabling LNG carriers to navigate at night can substantially reduce their waiting times when the port has a large ship visit volume, ultimately improving the overall scheduling efficiency (LinkedIn, 2023). Sensitivity analysis, focusing on LNG berth utilization during peak periods and the maximum number of LNG carriers able to navigate normally, underscores the practical benefits of night navigation. These include improved LNG berth resource utilization and enhanced port accessibility for LNG carriers, contributing to optimal port resource allocation and operational efficiency improvements.

This study provides a comprehensive framework for addressing the complexities of ship traffic scheduling in LNG port areas, focusing on minimizing waiting times while considering LNG carrier navigation constraints. Empirical results from Shenzhen Dapeng Bay indicate that allowing LNG carriers to navigate at night significantly improves scheduling efficiency by 22.24 % compared to the FCFS method. For port managers, the proposed methodology offers a decision-support tool to optimize ship traffic scheduling by dynamically adjusting ship entry and exit sequences. This approach enhances resource utilization by reducing peak-hour congestion and allows LNG carriers to be prioritized while maintaining operational safety. However, the proposed methodology is subject to certain limitations, which we plan to address in future work. These include the impact of meteorological and hydrological factors on scheduling decisions, as well as the need to balance port operation costs with scheduling efficiency, all while ensuring the safety of LNG carrier navigation. Future research will extend this work by incorporating additional optimization objectives, such as port operation costs and safety, to develop a multi-objective programming model. Regarding algorithm design, we plan to explore alternative optimization algorithms with better search performance and more efficient model-solving capabilities. These advancements aim to further evaluate the impact of LNG carrier navigation and night operations on port efficiency, offering theoretical and practical insights for port operation management.

Funding

The author(s) declare that financial support was received for the research, authorship, and/or publication of this article. This work is financially supported by the Guangdong Basic and Applied Basic Research Foundation of China (Grant No. 2022A1515110776), by the Philosophy and Social Sciences Planning Project of Guangdong Province under Grant GD24XGL066.

CRediT authorship contribution statement

Shengping Dong: Writing – review & editing, Validation, Supervision, Conceptualization. **Guangyao Yang:** Writing – original draft, Validation, Software, Investigation, Formal analysis. **Shiguan Liao:** Writing – review & editing, Supervision, Methodology, Data curation, Conceptualization. **Lu Li:** Writing – review & editing, Visualization, Validation, Software, Investigation.

Declaration of competing interest

The authors declare that they have no known competing financial interests or personal relationships that could have appeared to influence the work reported in this paper.

References

Abdussamie, N., Daboos, M., Elferjani, I., Shuhong, C., Alaktiwi, A., 2018. Risk assessment of LNG and FLNG vessels during manoeuvring in open sea. J. Ocean Eng. Sci. 3, 56–66.
Abou Kasm, O., Diabat, A., Bierlaire, M., 2021. Vessel scheduling with pilotage and tugging considerations. Transp. Res. Pt. e-Logist. Transp. Rev. 148, 102231.
Chen, Y.-Z., Shi, C.-L., Claudel, C.G., Hu, M.-B., 2023. First train timetable synchronization with interval trains in subway networks. Transportmetrica B-Transp. Dyn. 11, 69–92.
China National Standards, 2021. Design Code of LNG Terminal, vol. 165. JTS.
China Water Transportation Net, 2023. Loading and unloading at Shenzhen's Dapeng LNG hub port during the Spring Festival reached an all-time high [WWW Document]. URL. http://www.zgsyb.com/news.html?aid=643624.
Dulebenets, M.A., 2018. Green vessel scheduling in liner shipping: modeling carbon dioxide emission costs in sea and at ports of call. Int. J. Trans. Sci. Technol. 7, 26–44.
Engelen, S., Dullaert, W., 2010. Designing a decision support model for the LNG market. Transport. Plann. Technol. 33, 719–731.
Gan, S., Wang, Y., Li, K., Liang, S., 2021. Efficient online one-way traffic scheduling for restricted waterways. Ocean Eng. 237, 109515.
González Gutiérrez, C., Diaz-Ruiz-Navamuel, E., Herrero, A., Ortega-Piris, A., 2023. Assessing energy efficiency and regulatory complexity in steam-powered LNG carriers. Ocean Eng. 286, 115671.
Hill, A., Lalla-Ruiz, E., Voss, S., Goycoolea, M., 2019. A multi-mode resource-constrained project scheduling reformulation for the waterway ship scheduling problem. J. Sched. 22, 173–182.
Jia, Q., Li, R., Li, J., 2023. Departure vessel scheduling optimization considering traffic restrictions in turning basin: ATerminal case study for xuwen. J. Mar. Sci. Eng. 11, 1311.
Jiang, X., Zhong, M., Shi, J., Li, W., 2024. Optimization of integrated scheduling of restricted channels, berths, and yards in bulk cargo ports considering carbon emissions. Expert Syst. Appl. 255, 124604.
Jiang, X., Zhong, M., Shi, J., Li, W., Sui, Y., Dou, Y., 2022. Overall scheduling model for vessels scheduling and berth allocation for ports with restricted channels that considers carbon emissions. J. Mar. Sci. Eng. 10, 1757.
Karbassi Yazdi, A., Kaviani, M.A., Emrouznejad, A., Sahebi, H., 2020. A binary particle swarm optimization algorithm for ship routing and scheduling of liquefied natural gas transportation. Trans. Lett. 12, 223–232.
Lalla-Ruiz, E., Shi, X., Voss, S., 2018. The waterway ship scheduling problem. Transport. Res. Transport Environ. 60, 191–209.
Li, R., Zhang, X., Jiang, L., Yang, Z., Guo, W., 2022. An adaptive heuristic algorithm based on reinforcement learning for ship scheduling optimization problem. Ocean Coast Manag. 230, 106375.
Li, Z., Hu, S., Gao, G., Yao, C., Fu, S., Xi, Y., 2021b. Decision-making on process risk of Arctic route for LNG carrier via dynamic Bayesian network modeling. J. Loss Prev. Process. Ind. 71, 104473.
Li, S., Jia, S., 2019. The seaport traffic scheduling problem: formulations and a column-row generation algorithm. Transp. Res. Part B Methodol. 128, 158–184.
Li, X., Tang, W., 2019. Structural risk analysis model of damaged membrane LNG carriers after grounding based on Bayesian belief networks. Ocean Eng. 171, 332–344.
Li, J., Zhang, X., Yang, B., Wang, N., 2021a. Vessel traffic scheduling optimization for restricted channel in ports. Comput. Ind. Eng. 152, 107014.
LinkedIn, 2023. Exploring the concept and advantages of night navigation for Pakistan [WWW Document]. URL. https://www.linkedin.com/pulse/exploring-concept-advantages-night-navigation-pakistan.
Liu, B., Li, Z.-C., Wang, Y., Sheng, D., 2021b. Short-term berth planning and ship scheduling for a busy seaport with channel restrictions. Transp. Res. Pt. e-Logist. Transp. Rev. 154, 102467.
Liu, J., Liu, Y., Qi, L., 2021a. Modelling liquefied natural gas ship traffic in port based on cellular automaton and multi-agent system. J. Navig. 74, 533–548.
Liu, C., Smith-Miles, K., Wauters, T., Costa, A.M., 2024b. Instance space analysis for 2D bin packing mathematical models. Eur. J. Oper. Res. 315, 484–498.
Liu, K., Xin, X., Ma, J., Zhang, J., Yu, Q., 2019. Sensitivity analysis of ship traffic in restricted two-way waterways considering the impact of LNG carriers. Ocean Eng. 192, 106556.
Liu, S., Zhang, Y., Guo, W., Tian, H., Tang, K., 2024a. Ship scheduling problem based on channel-lock coordination in flood season. Expert Syst. Appl. 254, 124393.
Marroni, G., Casson Moreno, V., Ovidi, F., Chiavistelli, T., Landucci, G., 2023. A methodology for risk assessment of LNG carriers accessing vulnerable port areas. Ocean Eng. 273, 114019.
Meng, L., Wang, X., Jin, J., Han, C., 2023. Optimization model for container liner ship scheduling considering disruption risks and carbon emission reduction. J. Mar. Sci. Eng. 11, 1449.
Nam, H., Lee, T., 2013. A scheduling problem for a novel container transport system: a case of mobile harbor operation schedule. Flex. Serv. Manuf. J. 25, 576–608.
Ning, Y., Zhang, F., Jin, B., Wang, M., 2023. Three-dimensional path planning for a novel sediment sampler in ocean environment based on an improved mutation operator genetic algorithm. Ocean Eng. 289, 116142.
Nwaoha, T.C., Yang, Z., Wang, J., Bonsall, S., 2013. Adoption of new advanced computational techniques to hazards ranking in LNG carrier operations. Ocean Eng. 72, 31–44.
Peng, Y., Zhao, X., Zuo, T., Wang, W., Song, X., 2021. A systematic literature review on port LNG bunkering station. Transport. Res. Part D-Transport. Environ. Times 91, 102704.
Shen, L., Xu, X., Shao, F., Shao, H., Ge, Y., 2024. A multi-objective optimization model for medical waste recycling network design under uncertainties. Transp. Res. Pt. e-Logist. Transp. Rev. 184, 103492.
Tang, N., Wang, X., Gao, S., Ai, B., Li, B., Shang, H., 2024. Collaborative ship scheduling decision model for green tide salvage based on evolutionary population dynamics. Ocean Eng. 304, 117796.
Vanem, E., Antão, P., Østvik, I., de Comas, F.D.C., 2008. Analysing the risk of LNG carrier operations. Reliabil. Eng.; Syst. Saf., Saf. Maritime Trans. 93, 1328–1344.
Wang, H., Tian, W., Zhang, J., Li, Y., 2020. A hybrid self-organizing scheduling method for ships in restricted two-way waterways. Brodogradnja 71, 15–30.
Wang, S., Qi, J., Laporte, G., 2022. Governmental subsidy plan modeling and optimization for liquefied natural gas as fuel for maritime transportation. Transp. Res. Part B Methodol. 155, 304–321.
Wu, L., Adulyasak, Y., Cordeau, J.-F., Wang, S., 2022. Vessel service planning in seaports. Oper. Res. 70.
Xia, Z., Feng, T., Guo, Z., Jiang, Y., Wang, W., 2023. Research on safety and efficiency warranted vessel scheduling in unidirectional multi-junction waterways of port waters. Comput. Ind. Eng. 180, 109284.
Xiong, Z., Zhao, M., Tan, L., Cai, L., 2022. Real-time power optimization for application server clusters based on Mixed-Integer Programming. Future Gener. Comput. Syst. 137, 260–273.
Yang, W., Chen, X., Liu, Y., 2023. Review and reflections of legislation and policies on shipping decarbonization under China's "dual carbon" target. Front. Mar. Sci. 10, 1131552.
Yao, P., Duan, X., Tang, J., 2024. An improved gray wolf optimization to solve the multi-objective tugboat scheduling problem. PLoS One 19, e0296966.
Zhang, B., Zheng, Z., Wang, D., 2020. A model and algorithm for vessel scheduling through a two-way tidal channel. Marit. Pol. Manag. 47, 188–202.
Zhang, H., Ke, J., 2024. An intelligent scheduling system and hybrid optimization algorithm for ship locks of the three gorges hub on the yangtze river. Mech. Syst. Signal Process. 208, 110974.
Zhang, Y., Liu, S., Zheng, Q., Tian, H., Guo, W., 2024a. Ship scheduling problem in an anchorage-to-quay channel with water discharge restrictions. Ocean Eng. 309, 118432.
Zhang, J., Santos, T.A., Guedes Soares, C., Yan, X., 2017. Sequential ship traffic scheduling model for restricted two-way waterway transportation. Proc. Inst. Mech. Eng. Part M- J. Eng. Marit. Environ. 231, 86–97.
Zhang, X., Li, R., Wang, C., Xue, B., Guo, W., 2024b. Robust optimization for a class of ship traffic scheduling problem with uncertain arrival and departure times. Eng. Appl. Artif. Intell. 133, 108257.
Zheng, H., Wang, Z., Duan, S., 2025. Integrated optimization of vessel sequencing and bulk carrier berth allocation with shifting in a comprehensive port. Ocean Eng. 316, 119891.
Zhou, T., Wu, C., Zhang, J., Zhang, D., 2017. Incorporating CREAM and MCS into fault tree analysis of LNG carrier spill accidents. Saf. Sci. 96, 183–191.
Zhu, M., Huang, L., Huang, Z., Shi, F., Xie, C., 2022. Hazard analysis by leakage and diffusion in Liquefied Natural Gas ships during emergency transfer operations on coastal waters. Ocean Coast Manag. 220, 106100.